Texas A&M Transportation Institute

Test Report No. 622561

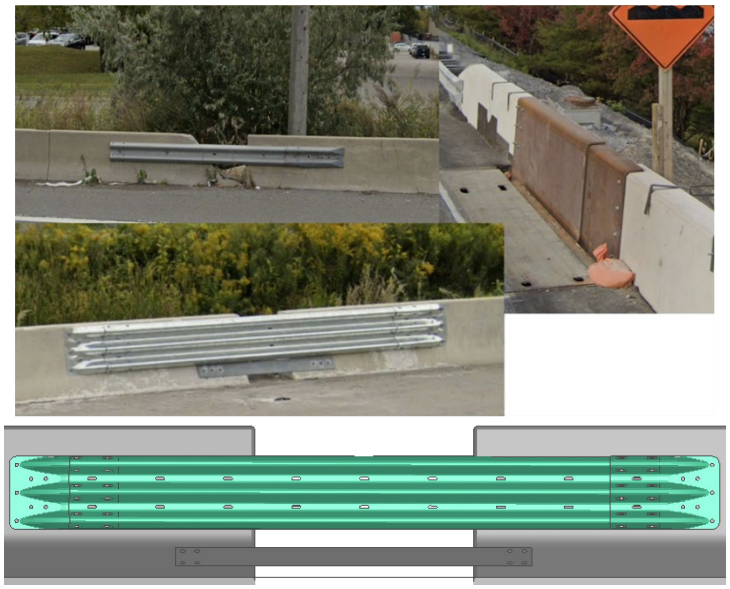

BRIDGING GAPS IN CONCRETE BARRIERS – PHASE 1

Sponsored by

WASHINGTON STATE DEPARTMENT OF TRANSPORTATION (WSDOT)

TEXAS A&M TRANSPORTATION INSTITUTE
Roadside Safety & Physical Security
Texas A&M University System
RELLIS Campus
Building 7091
1254 Avenue A
Bryan, TX 77807

Technical Report Documentation Page

1. Report No.	2. Government Accession No.	3. Recipient's Catalog No.
622561		

4. Title and Subtitle	5. Report Date
Bridging Gaps in Concrete Barriers - Phase 1	April 2026
	6. Performing Organization Code

7. Author(s)	8. Performing Organization Report No.
Sun Hee Park, William Williams, and Woojin Kim	TRNo. 620841

9. Performing Organization Name and Address	10. Work Unit No. (TRAIS)
Texas A&M Transportation Institute Proving Ground 3135 TAMU College Station, Texas 77843-3135	11. Contract or Grant No. Contract T1969-B3

12. Sponsoring Agency Name and Address	13. Type of Report and Period Covered
Washington State Department of Transportation Research Office MS 47372 Transportation Building Olympia, WA 98504-7372	Technical Report: April 2026
	14. Sponsoring Agency Code

15. Supplementary Notes

Name of Contacting Representative: [Kenneth Shannon, P. Eng.]

16. Abstract

Concrete barriers are prone to damage, which often results in gaps requiring prompt field repairs. Common interim solutions—such as W-beam guardrails, thrie beam guardrails, and steel plates—are frequently used by maintenance teams due to their cost-effectiveness and ease of installation. This project focused on developing a MASH Test Level 3 (TL-3) compliant bridging barrier gap design and established the maximum safe gap width between concrete barrier segments. The design concepts were based on the Ontario Tall Wall Median Barrier, utilizing a single 12-gauge thrie beam guardrail with a 6-inch steel rub rail plate installed at the base of an F-shape concrete barrier.

A finite element (FE) model was developed to evaluate performance across a range of gap widths (18 to 72 inches) in LS-DYNA impact simulations with both small car and pickup truck. Based on the simulation findings, the 60-inch gap was determined to be the maximum width at which the bridging barrier system likely pass the MASH TL-3 requirements for both small car and pickup truck.

17. Key Words	18. Distribution Statement
Concrete Barrier, LS-DYNA, Bridge Barrier, Gap, MASH, Longitudinal Barrier	No restrictions. This document is available to the public through NTIS: National Technical Information Service Alexandria, Virginia 22312 http://www.ntis.gov

19. Security Classification. (of this report)	20. Security Classification. (of this page)	21. No. of Pages	22. Price
Unclassified	Unclassified	39	

Form DOT F 1700.7 (8-72) Reproduction of completed page authorized.

Bridging Gaps in Concrete Barriers - Phase 1

By

Sun Hee Park, Ph.D.
Assistant Research Scientist
Texas A&M Transportation Institute

William Williams, P.E.
Associate Research Engineer
Texas A&M Transportation Institute

and

Woojin Kim.
Graduate Student Researcher
Texas A&M Transportation Institute

Report 622561
Contract No.: T1969-AN

Sponsored by the

Washington State Department of Transportation

April 2026

TEXAS A&M TRANSPORTATION INSTITUTE
College Station, Texas 77843-3135

DISCLAIMER

The contents of this report reflect the views of the authors, who are solely responsible for the facts and accuracy of the data and the opinions, findings, and conclusions presented herein. The contents do not necessarily reflect the official views or policies of the Roadside Safety Pooled Fund, The Texas A&M University System, or the Texas A&M Transportation Institute (TTI). This report does not constitute a standard, specification, or regulation. In addition, the above listed agencies/companies assume no liability for its contents or use thereof. The names of specific products or manufacturers listed herein do not imply endorsement of those products or manufacturers.

ACKNOWLEDGEMENTS

This research project was performed under a pooled fund program between the following States and Agencies. The authors acknowledge and appreciate their guidance and assistance.

Roadside Safety Research Pooled Fund Committee
Revised April 2024

ALABAMA

Wade Henry, P.E.
Assistant State Design Engineer
Design Bureau, Final Design Division
Alabama Dept. of Transportation
1409 Coliseum Boulevard, T-205
Montgomery, AL 36110
(334) 242-6464
henryw@dot.state.al.us

Stanley (Stan) C. Biddick, P.E.
State Design Engineer
Alabama Dept. of Transportation
1409 Coliseum Boulevard, T-205
Montgomery, AL 36110
(334) 242-6488
biddicks@dot.state.al.us

ALASKA

Mary F. McRae
Assistant State Traffic & Safety EngineerAlaska Depart. of Transportation & Public Facilities
3132 Channel Drive
P.O. Box 112500
Juneau, AK 99811-2500
(907) 465-6963
mary.mcrae@alaska.gov

Micheal Hills
Alaska Depart. of Transportation & Public Facilities
micheal.hills@alaska.gov

CALIFORNIA

Bob Meline, P.E.
Caltrans
Office of Materials and Infrastructure
Division of Research and Innovation
5900 Folsom Blvd
Sacramento, CA 95819
(916) 227-7031
Bob.Meline@dot.ca.gov

John Jewell, P.E.
Senior Crash Testing Engineer
Office of Safety Innovation & Cooperative Research
(916) 227-5824
John_Jewell@dot.ca.gov

COLORADO

David Kosmiski, P.E.
Miscellaneous (M) Standards Engineer
Division of Project Support, Construction Engineering Services (CES) Branch
Colorado Dept. of Transportation (CDOT)
2829 W. Howard Pl.
Denver, CO 80204
303-757-9021
david.kosmiski@state.co.us

Andy Pott, P.E.
Senior Bridge Design and Construction Engineer
Division of Project Support, Staff Bridge Design and Construction Management
Colorado Dept. of Transportation (CDOT)
4201 E Arkansas Ave, 4th Floor
Denver, CO 80222
303-512-4020
andrew.pott@state.co.us

Shawn Yu, P.E.
Miscellaneous (M) Standards and Specifications Unit Manager
Division of Project Support, Construction Engineering Services (CES) Branch
Colorado Dept. of Transportation (CDOT)
4201 E Arkansas Ave, 4th Floor
Denver, CO 80222
303-757-9474
shawn.yu@state.co.us

Amin Fakhimalizad
Assistant Miscellaneous (M) Standards Engineer
Division of Project Support, Construction Engineering Services (CES) Branch
Colorado Dept. of Transportation (CDOT)
303-757-9229
amin.fakhimalizad@state.co.us

Man (Steven) Yip
Division of Project Support, Construction Engineering Services (CES) Branch
Colorado Dept. of Transportation (CDOT)
man.yip@state.co.us

CONNECTICUT

David Kilpatrick
Transportation Supervising Engineer
State of Connecticut Depart. of Transportation
2800 Berlin Turnpike
Newington, CT 06131-7546
(806) 594-3288
David.Kilpatrick@ct.gov

Todd Ingarra
todd.ingarra@ct.gov

DELAWARE

Cassidy Blowers
Construction Resource Engineer
Construction Section
Delaware DOT
(302)760-2336
Cassidy.Blowers@delaware.gov

James Osborne
Traffic Safety Programs Manager
Traffic Operations
Delaware DOT
(302)659-4651
James.Osborne@delaware.gov

FLORIDA

Richard Stepp
Florida Department of Transportation
Richard.Stepp@dot.state.fl.us

Derwood C. Sheppard, Jr., P.E.
State Roadway Design Engineer
Florida Depart. of Transportation
Roadway Design Office
605 Suwannee Street, MS-32
Tallahassee, FL 32399-0450
(850) 414-4334
Derwood.Sheppard@dot.state.fl.us

IDAHO

Marc Danley, P.E.
Technical Engineer
(208) 334-8558
Marc.danley@itd.idaho.gov

Kevin Sablan
Design/Traffic Engineer
Idaho Transportation Department
(208) 334-8558
Kevin.sablan@itd.idaho.gov

ILLINOIS

Martha A. Brown, P.E.
Safety Design Bureau Chief
Bureau of Safety Programs and Engineering
Illinois Depart. of Transportation
2300 Dirksen Parkway, Room 005
Springfield, IL 62764
(217) 785-3034
Martha.A.Brown@illinois.gov

Edgar A. Galofre, MSCE, P.E.
Safety Design Engineer
Bureau of Safety Programs and Engineering
Illinois Department of Transportation
2300 S. Dirksen Parkway, Room 007
Springfield, IL 62764
(217) 558-9089
Edgar.Galofre@illinois.gov

IOWA

Daniel Harness
Design Bureau – Methods Section
Iowa Department of Transportation
Daniel.Harness@iowadot.us

Chris Poole
State Traffic Engineer
Traffic and Safety Bureau
Iowa Department of Transportation
Chris.Poole@iowadot.us

LOUISIANA

Carl Gaudry
Bridge Design Manager
Louisiana Department of Transportation and Development
Bridge & Structural Design Section
P.O. Box 94245
Baton Rouge, LA 70804-9245
(225) 379-1075
Carl.Gaudry@la.gov

Chris Guidry
Assistant Bridge Design Administrator
Louisiana Department of Transportation and Development
Bridge & Structural Design Section
P.O. Box 94245
Baton Rouge, LA 79084-9245
(225) 379-1328
Chris.Guidry@la.gov

MARYLAND

Philip Brentlinger
Maryland State Highway Administration
pbrentlinger@mdot.maryland.gov

MASSACHUSETTS

James Danila
Assistant State Traffic Engineer
Massachusetts Depart. of Transportation
(857) 368-9640
James.danila@state.ma.us

Alex Bardow
Director of Bridges and Structure
Massachusetts Depart. of Transportation
10 Park Plaza, Room 6430
Boston, MA 02116
(857) 368-9430
Alexander.Bardow@state.ma.us

MICHIGAN

Carlos Torres, P.E.
Roadside Safety Engineer
Geometric Design Unit, Design Division
Michigan Depart. of Transportation
P. O. Box 30050
Lansing, MI 48909
(517) 335-2852
TorresC@michigan.gov

MINNESOTA

Khamsai Yang
Design Standards Engineer
Office of Project Management and Technical Support
(612) 322-5601
Khamsai.Yang@state.mn.us

Brian Tang
Assistant Design Standards Engineer
Office of Project Management and Technical Support
Minnesota Department of Transportation
brian.tang@state.mn.us

MISSOURI

Gidget Koestner
Policy & Innovations Engineer
Central Office- Design
Missouri Department of Transportation
(573) 751-6905
gidget.koestner@modot.mo.gov

Kirby Woods
Roadside Design Engineer
Missouri Department of Transportation
(573) 472-5333
kirby.woodsjr@modot.mo.gov

NEW MEXICO

Brad Julian
New Mexico Department of Transportation
Traffic Technical Support Engineer
(505) 469-1405
Brad.Julian@dot.nm.gov

NEVADA

David Fox, P.E.
Specifications Engineer
Roadway Design Division
Nevada Dept. of Transportation
1263 S. Stewart St.
Carson City, NV 89712
(775) 888-7053
DWFox@dot.nv.gov

Tim Rudnick
Standards and Manuals Supervisor
Roadway Design Division
Nevada Dept. of Transportation
1263 S. Stewart St.
Carson City, NV 89712
(775) 888-7598
TRudnick@dot.nv.gov

OHIO

Don P. Fisher, P.E.
Ohio Depart. of Transportation
1980 West Broad Street
Mail Stop 1230
Columbus, OH 43223
(614) 387-2614
Don.fisher@dot.ohio.gov

OREGON

Christopher Henson
Senior Roadside Design Engineer
Oregon Depart. of Transportation
Technical Service Branch
4040 Fairview Industrial Drive, SE
Salem, OR 97302-1142
(503) 986-3561
Christopher.S.Henson@odot.state.or.us

PENNSYLVANIA

James A. Borino, Jr., P.E.
Chief, Standards and Criteria Unit
Highway Design and Technology Division
Pennsylvania DOT
(717) 612-4791
jborino@pa.gov

Evan Pursel
Senior Civil Engineer
Highway Design and Technology Division
Pennsylvania DOT
(717) 705-8535
epursel@pa.gov

Nina Ertel
Project Development Engineer
Highway Design and Technology Division
Pennsylvania DOT
(717) 425-7679
nertel@pa.gov

TENNESSEE

Laura Chandler
Engineering Production Support Manager
Engineering Division
Tennessee Dept. of Transportation
(615) 253-4769
Laura.Chandler@tn.gov

Ali Hangul M.S., P.E
State Standards Transportation Engineer
Engineering Production Support,
Engineering Division
Tennessee Dept. of Transportation
(615) 741-0840
Ali.Hangul@tn.gov

TEXAS

Chris Lindsey
Transportation Engineer
Design Division
Texas Department of Transportation
125 East 11th Street
Austin, TX 78701-2483
(512) 416-2750
Christopher.Lindsey@txdot.gov

Taya Retterer
TxDOT Bridge Standards Engineer
Bridge Division
Texas Department of Transportation
(512) 993-0330
Taya.Retterer@txdot.gov

Wade Odell
Research Project Manager
Research & Technology Implementation Division
Texas Department of Transportation
(512) 416-4737
wade.odell@txdot.gov

UTAH

Clint McCleery
Barrier and Attenuation Specialist
Traffic and Safety Operations
Utah Department of Transportation
(801)712-8685
cmccleery@utah.gov

WASHINGTON

Tim Moeckel
Roadside Safety Engineer
Washington State Department of Transportation
Development Division
P.O. Box 47329
Olympia, WA 98504-7246
(360) 704-6377
moecket@wsdot.wa.gov

Mustafa Mohamedali
Research Manager/Engineering
Transportation Safety & System Analysis
Research & Library Services
(360) 704-6307
mohamem@wsdot.wa.gov

Kevin Burch
Policy Support Engineer
Washington State Department of Transportation
Development Division
burchk@wsdot.wa.gov

WEST VIRGINIA

Donna J. Hardy, P.E.
Mobility, ITS & Safety Engineer
West Virginia Depart. of Transportation – Traffic Engineering
Building 5, Room A-550
1900 Kanawha Blvd E.
Charleston, WV 25305-0430
(304) 414-7338
Donna.J.Hardy@wv.gov

Ted Whitmore
Traffic Services Engineer
Traffic Engineering
WV Division of Highways
(304)414-7373
Ted.J.Whitmore@wv.gov

WISCONSIN

Erik Emerson, P.E.
Standards Development Engineer – Roadside Design
Wisconsin Department of Transportation
Bureau of Project Development
4802 Sheboygan Avenue, Room 651
P. O. Box 7916
Madison, WI 53707-7916
(608) 266-2842
Erik.Emerson@wi.gov

CANADA – ONTARIO

Kenneth Shannon, P. Eng.
Senior Engineer, Highway Design (A)
Ontario Ministry of Transportation
301 St. Paul Street
St. Catharines, ON L2R 7R4
CANADA
(904) 704-3106
Kenneth.Shannon@ontario.ca

FEDERAL HIGHWAY ADMINISTRATION (FHWA)

Website: safety.fhwa.dot.gov

Eduardo Arispe
Research Highway Safety Specialist
U.S. Department of Transportation
Federal Highway Administration
Turner-Fairbank Highway Research Center
Mail Code: HRDS-10
6300 Georgetown Pike
McLean, VA 22101
(202) 493-3291
Eduardo.arispe@dot.gov

Richard B. (Dick) Albin, P.E.
Senior Safety Engineer
Office of Innovation Implementation, Safety & Design Team
(303) 550-8804
Dick.Albin@dot.gov

Paul LaFleur, P.E.
Safety Design Team - Roadway Departure Program Manager
FHWA Office of Safety
U.S. Department of Transportation
(515) 233-7308
paul.lafleur@dot.gov

Christine Black
Highway Safety Engineer
Central Federal Lands Highway Division
12300 West Dakota Ave.
Lakewood, CO 80228
(720) 963-3662
Christine.black@dot.gov

Isbel Ramos-Reyes
Lead Safety and Transportation Operations Engineer
Eastern Federal Lands Highway Division
(703) 948-1442
isbel.ramos-reyes@dot.gov

TEXAS A&M TRANSPORTATION INSTITUTE (TTI)

Website: tti.tamu.edu
www.roadsidepooledfund.org

D. Lance Bullard, Jr., P.E.
Senior Research Engineer
Roadside Safety & Physical Security Div.
Texas A&M Transportation Institute
3135 TAMU
College Station, TX 77843-3135
(979) 317-2855
L-Bullard@tti.tamu.edu

Roger P. Bligh, Ph.D., P.E.
Senior Research Engineer
Roadside Safety and Physical Security Division
(979) 317-2703
R-Bligh@tti.tamu.edu

Nauman Sheikh, P.E.
Research Engineer
Roadside Safety and Physical Security
Texas A&M Transportation Institute
(979) 317-2703
n-sheikh@tti.tamu.edu

Ariel Sheil
Research Assistant
Roadside Safety and Physical Security
Texas A&M Transportation Institute
(979) 317-2250
A-Sheil@tti.tamu.edu

TABLE OF CONTENTS

LIST OF FIGURES

LIST OF TABLES

SI* (MODERN METRIC) CONVERSION FACTORS				
APPROXIMATE CONVERSIONS TO SI UNITS				
Symbol	**When You Know**	**Multiply By**	**To Find**	**Symbol**
		LENGTH		
in	inches	25.4	millimeters	mm
ft	feet	0.305	meters	m
yd	yards	0.914	meters	m
mi	miles	1.61	kilometers	km
		AREA		
in^2	square inches	645.2	square millimeters	mm^2
ft^2	square feet	0.093	square meters	m^2
yd^2	square yards	0.836	square meters	m^2
ac	acres	0.405	hectares	ha
mi^2	square miles	2.59	square kilometers	km^2
		VOLUME		
fl oz	fluid ounces	29.57	milliliters	mL
gal	gallons	3.785	liters	L
ft^3	cubic feet	0.028	cubic meters	m^3
yd^3	cubic yards	0.765	cubic meters	m^3
	NOTE: volumes greater than 1000L shall be shown in m^3			
		MASS		
oz	ounces	28.35	grams	g
lb	pounds	0.454	kilograms	kg
T	short tons (2000 lb)	0.907	megagrams (or metric ton")	Mg (or "t")
		TEMPERATURE (exact degrees)		
°F	Fahrenheit	5(F-32)/9 or (F-32)/1.8	Celsius	°C
		FORCE and PRESSURE or STRESS		
lbf	poundforce	4.45	newtons	N
lbf/in^2	poundforce per square inch	6.89	kilopascals	kPa
APPROXIMATE CONVERSIONS FROM SI UNITS				
Symbol	**When You Know**	**Multiply By**	**To Find**	**Symbol**
		LENGTH		
mm	millimeters	0.039	inches	in
m	meters	3.28	feet	ft
m	meters	1.09	yards	yd
km	kilometers	0.621	miles	mi
		AREA		
mm^2	square millimeters	0.0016	square inches	in^2
m^2	square meters	10.764	square feet	ft^2
m^2	square meters	1.195	square yards	yd^2
ha	hectares	2.47	acres	ac
km^2	Square kilometers	0.386	square miles	mi^2
		VOLUME		
mL	milliliters	0.034	fluid ounces	oz
L	liters	0.264	gallons	gal
m^3	cubic meters	35.314	cubic feet	ft^3
m^3	cubic meters	1.307	cubic yards	yd^3
		MASS		
g	grams	0.035	ounces	oz
kg	kilograms	2.202	pounds	lb
Mg (or "t")	megagrams (or "metric ton")	1.103	short tons (2000lb)	T
		TEMPERATURE (exact degrees)		
°C	Celsius	1.8C+32	Fahrenheit	°F
		FORCE and PRESSURE or STRESS		
N	newtons	0.225	poundforce	lbf
kPa	kilopascals	0.145	poundforce per square inch	lb/in^2

*SI is the symbol for the International System of Units

CHAPTER 1.

INTRODUCTION

1.1. BACKGROUND

Concrete barriers frequently sustain damage due to vehicle collisions or other incidents, resulting in openings that must be addressed to restore barrier integrity. In such situations, maintenance personnel commonly utilize readily available materials—including W-beam guardrail, thrie beam guardrail, and steel plates—to span localized gaps as temporary repairs (see Figure 1.1). These solutions provide a cost-effective and straightforward method for field construction, ensuring timely remediation while minimizing installation complexity.

It is important that these temporary repairs not only facilitate rapid and economical installation, but also maintain compliance with established crashworthiness standards, such as the Manual for Assessing Safety Hardware (MASH) [1] Test Level 3 (TL-3) criteria. The objective of this project is to evaluate the maximum gap or span that can be safely closed within a concrete barrier using standard and readily available hardware, with particular attention to ensuring performance that meets MASH TL-3 requirements.

Figure 1.1. Retrofits for Bridging Gaps in Concrete Barriers

1.2. OBJECTIVE

The scope of this initial phase is confined to engineering analyses and computational simulations utilizing LS-DYNA; full-scale crash testing is not included at this stage. Design development is founded on the Ontario Tall Wall Median Barrier, with pertinent cross-sectional details presented in Figure 1.2.

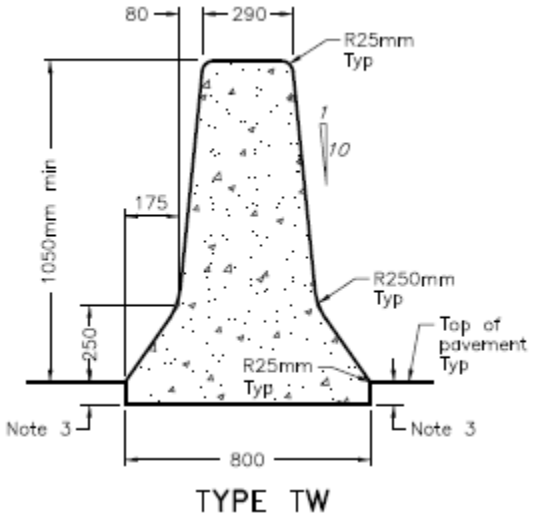

Figure 1.2 Details of Ontario Tall Wall Median Barrier

For the purpose of design evaluation, a single (non-nested) 12-gauge thrie beam guardrail has been selected as the primary element to span the opening in the F-shape concrete barrier. Additionally, a 6-inch anchored steel strap plate will be installed at the base of the barrier to enhance structural security across the gap. Representative photographs of the retrofit configurations considered in this study are shown in Figure 1.1.

A key objective of this phase is to determine the maximum allowable gap or span in a concrete barrier that can be effectively bridged using standard, readily available hardware, while continuing to meet the requirements of MASH TL-3. All investigations within this phase was conducted through computer simulations using LS-DYNA [2].

1.3. BENEFITS

The retrofit design that can span an opening in a concrete barrier (maximum span limit) that meets the performance requirements of MASH Test Level 3.

CHAPTER 2.

LITERATURE REVIEW

2.1. INTRODUCTION

In this chapter, previous studies and tested systems that connect gaps between concrete barriers are comprehensively reviewed. The focus is on the wide range of approaches and design solutions developed to address challenges in barrier transitions, constrained installations, and large joint connections. Through this review, the chapter highlights key components to span-over/manage gaps in concrete barrier systems across different roadway applications and its limitations.

2.2. TRANSITION BETWEEN TEMPORARY BARRIER TO PERMANENT CONCRETE MEDIAN BARRIER [3]

Wiebelhaus et al. [3] conducted a research study to develop a crashworthy transition between free-standing F-shape temporary concrete barriers and a rigid California single-slope permanent concrete median barrier. The connection system utilized a dual nested thrie-beam (either 12-gauge or 10-gauge) bolted across the joint between the barriers using five 3/4-inch diameter wedge-bolt anchors. Additionally, the system featured a sloped steel transition cap designed to bridge the 10-inch height difference between the 32-inch temporary barriers and the 42-inch permanent barrier. To manage the stiffness transition, the barriers adjacent to the permanent barrier were anchored to the roadway using an asphalt pin tie-down system featuring 1.5-inch diameter steel pins. These pins were installed in the holes on both the front and back faces of the barriers in the transition section. Figure 2.1whos the transition system before conducting tests.

However, the transition was specifically designed for the Kansas F-shape temporary barrier. Therefore, adaptation to other temporary barrier systems or different joint designs would require further study. Furthermore, while the system can be adjusted for different heights, the steel transition cap is mandatory for any permanent barrier taller than 32 inches.

Figure 2.1. Transition Between Temporary Barrier to Permanent Concrete Median Barrier using Thrie-Beam [3]

2.3. MANITOBA CONSTRAINED-WIDTH, TALL WALL BARRIER [4]

Rosenbaugh et al. [4] designed and performed tests on a 49.25-inch tall, single-slope concrete barrier system intended for bridge rail, median, and roadside applications. To accommodate the expansion and contraction joints required for bridge applications, the system utilizes a 6.625-inch open gap shielded by a 13-mm thick steel cover plate. This cover plate was bolted to the upstream side of the rail to allow for movement while preventing vehicle snagging on the exposed barrier ends. Figure 2.2 shows close view of the tested system with the steel cover plate.

For transitions between different barrier configurations, such as connecting a TL-5 median barrier to a TL-4 single-slope barrier, the study employed smooth dowel bars. These three 25-mm diameter plain dowels were placed through the barrier centerline to facilitate shear load transfer across the joints. The system's geometry was optimized to resist a minimum design load of 190 kips while minimizing the amount of steel reinforcement.

However, the treatments were also specially designed to bridge gaps spanning large sign support structures, and it was determined not to be TL-5 or TL-3 crashworthy, providing only limited safety for low-severity impacts. For real-world bridge installations, expansion joint gaps exceeding 12 inches were not evaluated and would require cantilevered barrier extensions to reduce the unsupported span.

Figure 2.2. Steel Cover Plate Shielding Gaps Between Concrete Barriers [4]

2.4. PCB STEEL COVER PLATE FOR LARGE OPEN JOINTS - PHASE I AND PHASE II [5, 6]

MwRSF [5, 6] developed portable concrete barriers (PCB) steel cover plated for large open joints. The research work was conducted under two individual phases. Under Phase I, design concepts were developed to shield longitudinal gaps in F-shape PCBs ranging from 6 inches to 12.5 feet, and evaluated the design using computer simualtions.

The preferred connection system design was a nested thrie-beam rail with a steel toe plate and internal lateral stiffeners. The thrie-beams were designed to be secured to the PCBs using terminal connectors and wedge bolt anchors, effectively spanning the gap without requiring barrier overlaps. The design uses two nested 12.5-ft long, 12-gauge thrie-beams with a 5/8-inch thick toe plate and three welded 1/4-inch stiffeners between the parallel rail sections. The toe plate is attached to the lower sloped face of the PCB segments to mitigate wheel snag on the rigid concrete ends. This configuration was intended to provide shear and tensile load transfer across the gap, maintaining the continuity of the free-standing barrier system. Simulations indicated that certain impact points on a 12.5-ft gap could lead to vehicle instability or rollover, requiring further design refinements of the toe plate to manage wheel snag.

Based on the Phase I findings, Phase II performed full-scale MASH TL-3 crash testing on the stiffened, thrie-beam gap-spanning hardware. The tested system utilized two nested 12-gauge thrie-beams, a 5/8-inch thick steel toe plate, and internal steel lateral spacers constructed of 1/4-inch thick steel plate. The hardware was anchored to the concrete barriers using 3/4-inch diameter wedge bolt anchors and 10-gauge thrie-beam terminal connectors. Figure 2.3 shows the photos for the tested system.

The testing validated that the hardware could safely redirect a 2270P pickup truck while limiting dynamic barrier deflection. The system was successful in transferring shear and tensile loads across variable gap lengths, ranging from 6 inches to a full 12.5-foot segment length. The final recommendations for installation involve varying the number of internal stiffeners based on the specific length of the longitudinal gap being spanned.

However, the system's usage is strictly limited to the Midwest F-shape PCB system and should not be applied to other joint designs or barrier shapes without further analysis. To maintain redirective performance, the system requires a minimum of eight PCB segments installed both upstream and downstream of the gap. Furthermore, the study was focused on work-zone applications and did not evaluate the long-term structural or maintenance performance of the hardware as a permanent median or bridge barrier attachment.

Figure 2.3. Bridging Large Opening Joints Between PCBs using Thrie-Beams and Steel Toe Plates [5, 6]

2.5. SUMMARY

The designs for connecting barrier gaps were reviewed and their limitations thoroughly investigated to guide the development of effective gap-bridging systems for permanent concrete barriers. The studies revealed that many existing systems are tailored to specific barrier shapes and are often restricted to use in median or temporary applications rather than for permanent installations. The analysis also highlighted limitations that the effectiveness of gap-bridging hardware in portable barriers depends on minimum barrier run lengths to provide sufficient resistance, and specialized treatments

for spanning large gaps or obstructions do not always meet crashworthiness standards. Importantly, long-term structural performance and maintenance considerations have not been fully addressed in current designs, indicating a need for further research and innovation in permanent gap-bridging systems for concrete barriers.

CHAPTER 3.

FINITE ELEMENT ANALYSIS

3.1. INTRODUCTION

This chapter provides a description of the finite element (FE) simulation conducted to evaluate the performance of the proposed bridging concrete barrier gap design in accordance with MASH Tests 3-10 and 3-11 specifications.

3.2. FINITEE ELEMNT (FE) MODELING

To conduct impact simulations for the performance evaluation using LS-DYNA, the FE model for the bridging gap design was developed with a pre-designed gap between the barriers.

3.2.1. Proposed Design

A solution for bridging gaps between concrete barriers was proposed and designed based on 1050 mm Ontario Tall Wall design (see Figure 1.2). The proposed design solution utilizes a 12-gauge thrie-beam to connect the barriers and to redirect vehicles with a ¼ inches thick rub rail plate to avoid tire snagging. The details of the design are shown in Figure 3.1. Depending on the gap width (X in Figure 3.1), the lengths of the thrie-beam and the rub rail plate are determined. If the gap width is wider than 48 inches, 12 ft 6 inches long thrie beam will be used; otherwise, 6 ft 3 inches long thrie beam will be used for the gap is equal or narrower than 48 inches. The rub rail plate length will be determined based on the gap width (X) with additional 16 inches for each side; the overall length of the rub rail plate will be "X+32 inches." To anchor the thrie-beam on the concrete barrier faces, an end-shoe is applied to each end with five threaded rods, while the rub rail plate is directly anchored to the concrete barrier.

To represent the most critical scenario in the finite element model, the concrete barriers were modeled as rigid elements, while steel parts, such as thrie-beams, rub rail plates, and end-shoes, were modeled by shell elements with corresponding thickness and steel material properties. The anchors were not geometrically modeled; instead, they were modeled with nodal rigid connections. The ground was also modeled as rigid elements since the contact between barrier embedment and the ground was not the main concern. After the model was developed, impact simulations for MASH Tests 3-10 and 3-11 were performed on this FE model using a pickup truck and a small car FE model.

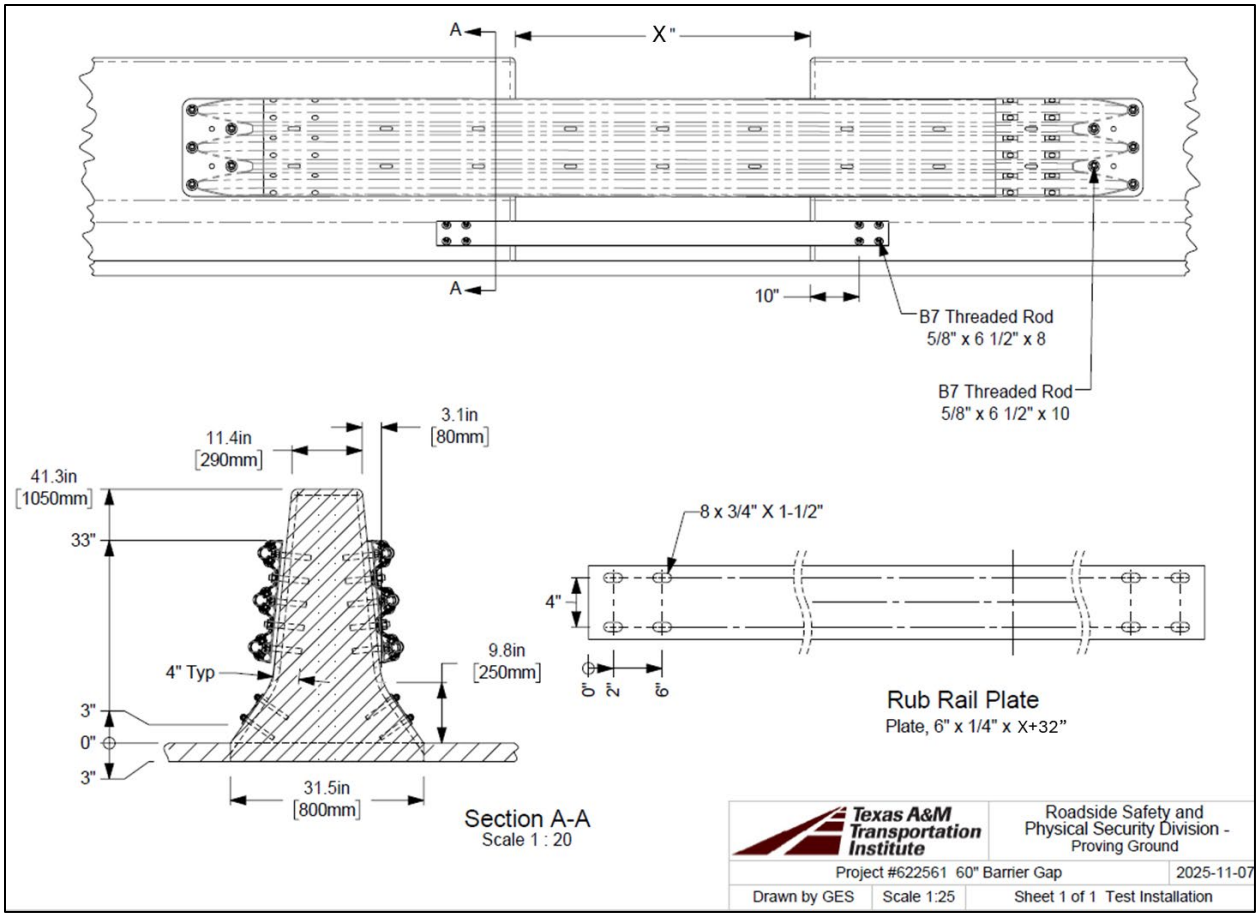

Figure 3.1. Proposed Design for Bridging Concrete Barrier Gap

3.2.2. Vehicle models

For the impact simulations, the research team used a 2018 Dodge Ram pickup truck model and a 2010 Toyota Yaris small car model [8,9], which are publicly available and were developed by the Center for Collision Safety and Analysis (CCSA) at George Mason University. These vehicle models have been further improved by TTI researchers over the course of various research projects to achieve greater validation and robustness. Figure 3.2 shows the pickup truck and small car models, which represent the MASH 2700P for MASH Test 11 and 1100C for MASH Test 10 design vehicles, respectively.

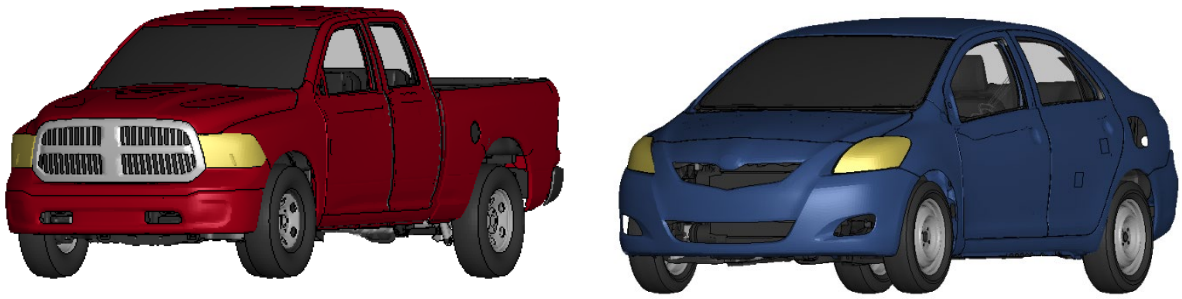

(a) 2018 Dodge Ram – MASH 2270P model (b) 2010 Toyota Yaris – MASH 1100C model

Figure 3.2. FE Vehicle Models.

3.3. IMPACT ANALYSIS

Simulations were performed on a range of gap widths (18 inches, 24 inches, 36 inches, 48 inches, 60 inches, 72 inches, etc.) to determine a critical/maximum width that exceeds the MASH requirements. Based on the simulations, the most critical gap width with the proposed bridging gap design will be recommended for full-scale crash testing in Phase 2 to be performed under a different project.

The performance of the bridging gap system was evaluated by impact analysis. In accordance with MASH TL-3 test conditions, the impact speed and angle were set as 62 mph and 25 degrees, respectively.

3.3.1. Critical Impact Point

The critical impact point (CIP) was determined based on MASH [1] as shown in Figure 3.3. MASH Table 2-7 for rigid barrier tests was used since the main system consists of concrete barriers, and steel parts (non-rigid) are only applied to connect the gaps between the rigid barriers.

To perform Tests 3-10 and 3-11, the CIPs were determined as 3.6 ft and 4.3 ft upstream, respectively, from a reference point. In this study, the reference point was selected as the middle of the thrie-beam to represent the most critical behavior accompanying the largest deflection on the beam. Therefore, the CIP for Test 3-10 and Test 3-11 was 3.6 ft and 4.3 ft upstream point, respectively, from the middle of the thrie-beam. Although the gap width between the concrete barriers was subjected to change, the CIP was not changed since the reference point was on the thrie-beam, not on the concrete barriers.

TABLE 2-7. Critical Impact Point for Rigid Barrier Tests with 1100C and 2270P Vehicles

Test Designation[a]	X Distance,[b] ft (m)
1-10, 2-10	3.3 (1.0)
3-10, 4-10, 5-10, 6-10	3.6 (1.1)
1-11, 2-11	2.6 (0.8)
3-11, 4-11, 5-11, 6-11	4.3 (1.3)

a See Table 2-2A for test details.
b See Figure 2-1 for illustration of x distance.

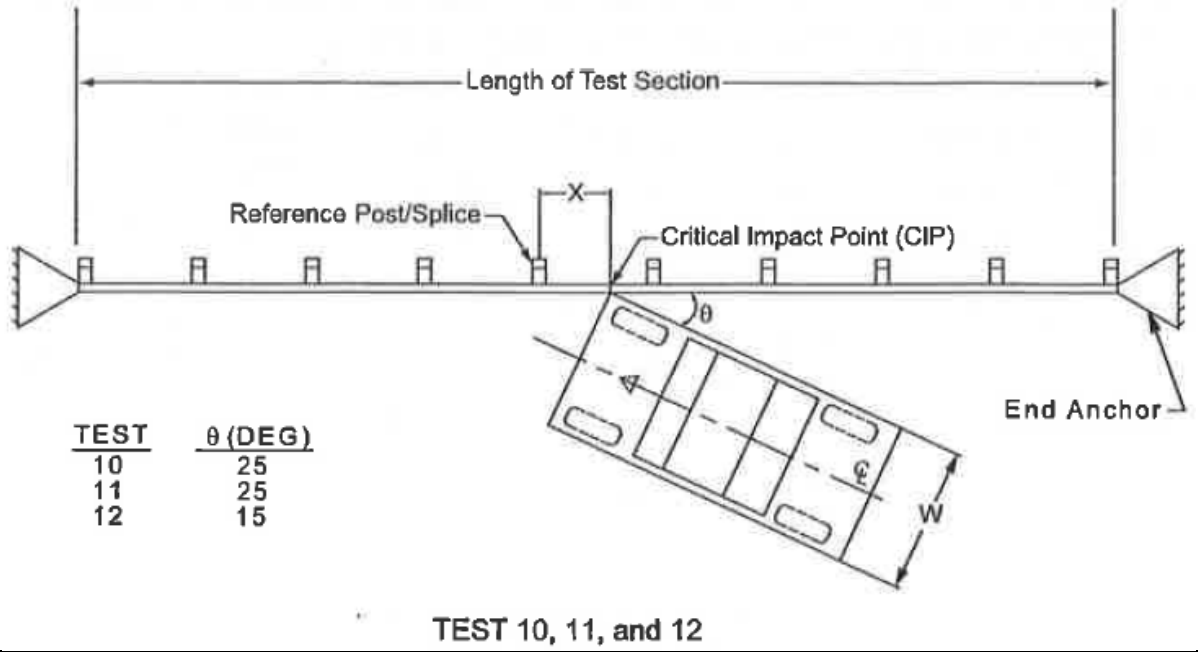

TEST 10, 11, and 12

Figure 3.3. Determine Critical Impact Point for Rigid Barrier Tests (MASH Figure 2-1 and Table 2-7) [1].

3.3.2. 18-inch Gap

The impact simulation was performed on the concrete barrier system with an 18-inch gap between the barriers. Figure 3.5 shows the FE model and vehicle setups showing the impact points and impact angles for Test 3-10 (small car) and Test 3-11 (pickup truck).

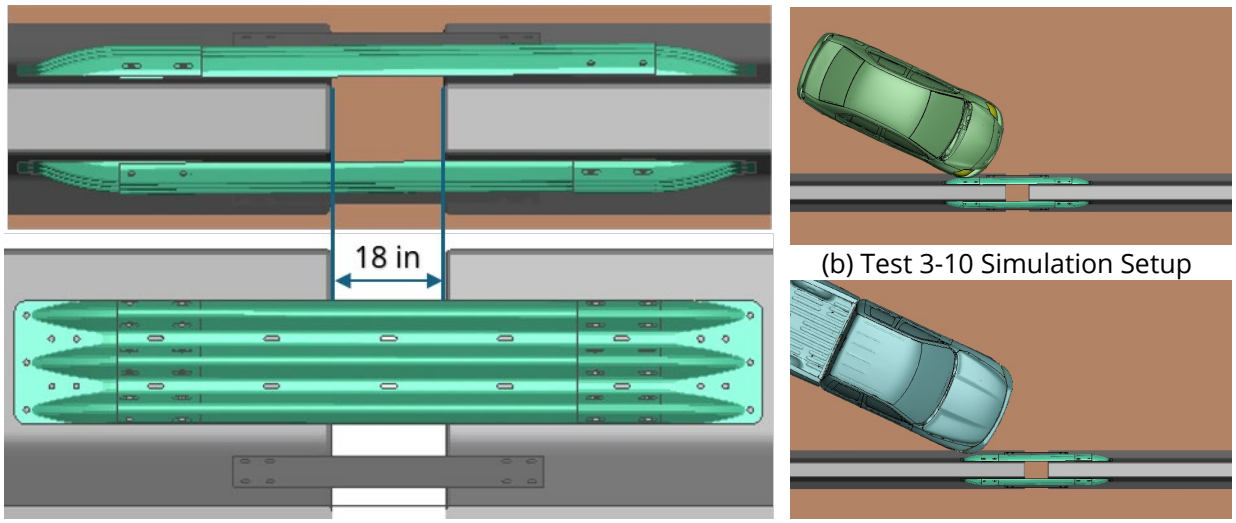

(a) Overview for 18-inch Gap Bridging

(b) Test 3-10 Simulation Setup

(c) Test 3-11 Simulation Setup

Figure 3.4. Bridging 18-inch Barrier Gap FE Model and Test Simulation Setup

Figure 3.5 and Figure 3.6 show sequential images capturing how the small car and pickup truck interact with the barrier system during the impact. Both vehicles were stably contained and redirected after impacting the system. Table 3.1 lists the occupant risk factors calculated using TRAP (Test Risk Assessment Program) [10]. All occupant risk factors from both impact simulations were under MASH limits. The bridging system with an18-inch width gap demonstrates great performance in terms of containment, redirection, and occupant safety.

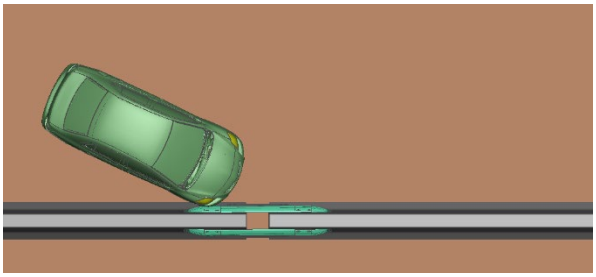

0.00 sec

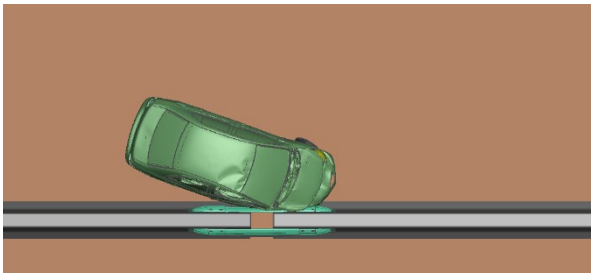

0.07 sec

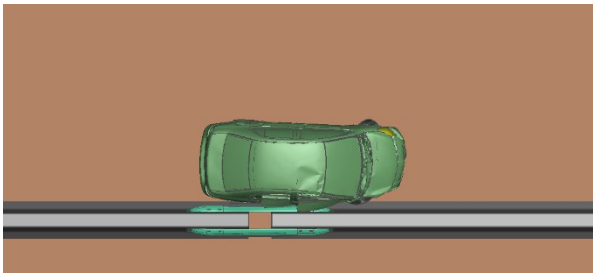

0.14 sec

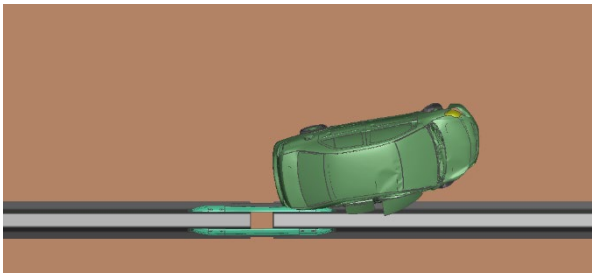

0.21 sec

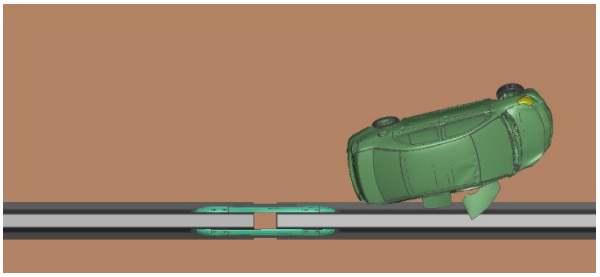

0.28 sec

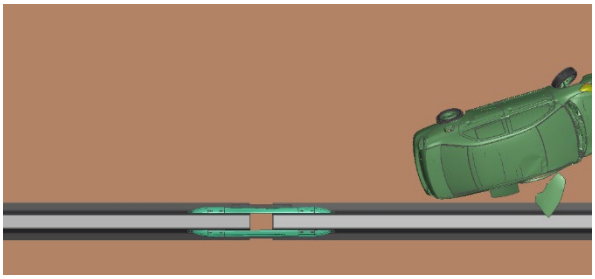

0.35 sec

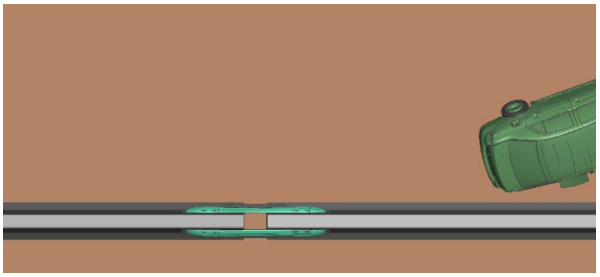

0.42 sec

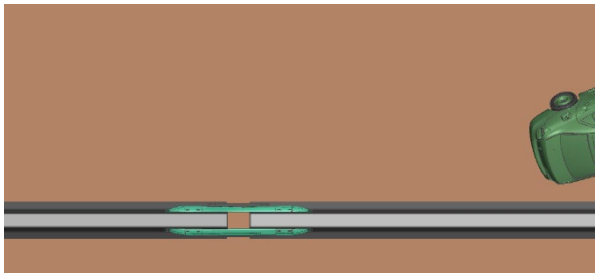

0.49 sec

Figure 3.5. Sequential Images for Test 3-10 Simulation with 18-inch Gap

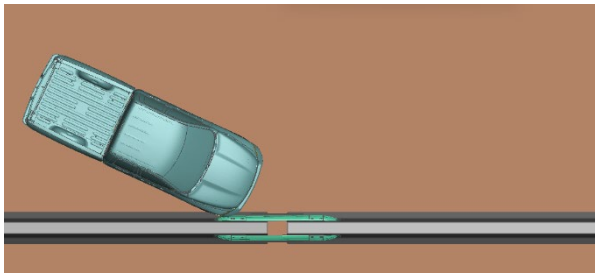

0.00 sec

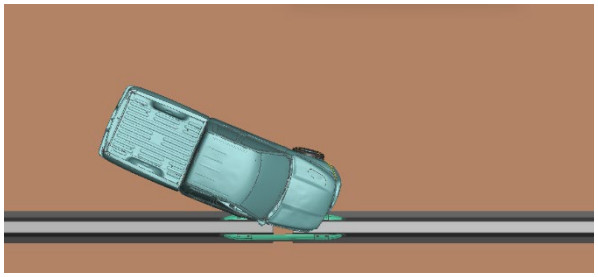

0.07 sec

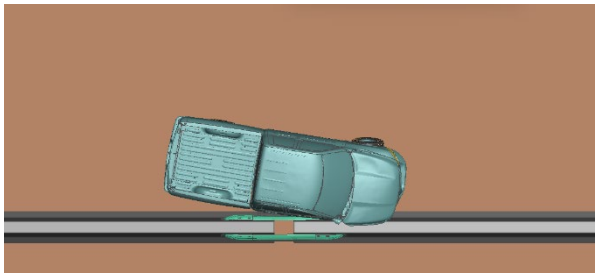

0.14 sec

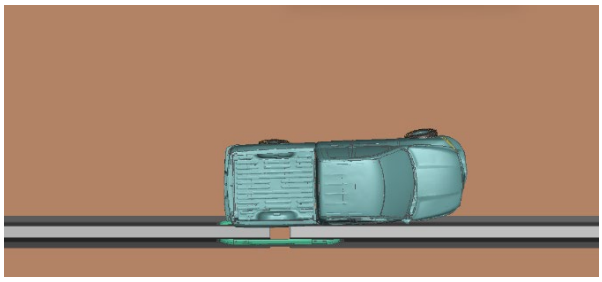

0.21 sec

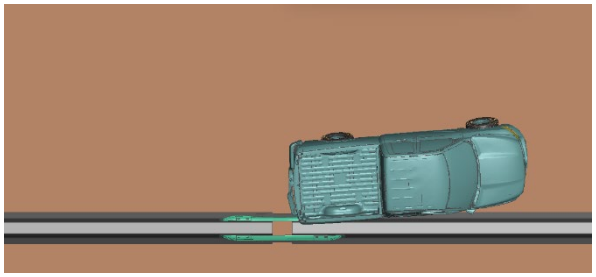

0.28 sec

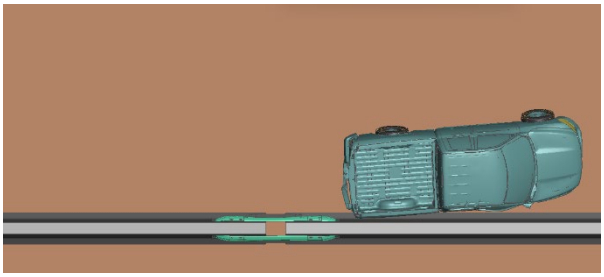

0.35 sec

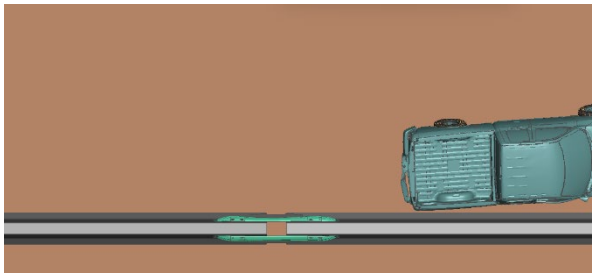

0.42 sec

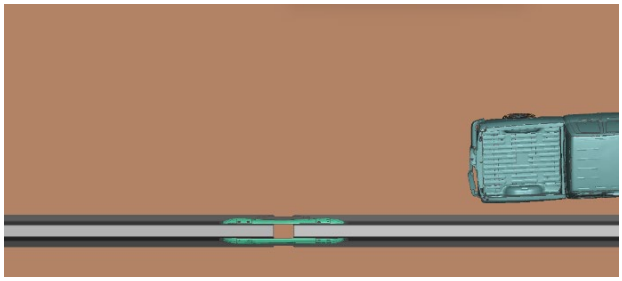

0.49 sec

Figure 3.6. Sequential Images for Test 3-11 Simulation with 18-inch Gap

Table 3.1. Occupant Risk Factors for 18-inch Gap Simulation Tests

Occupant Risk Factors		Small car	Pickup Truck
Occupant Impact Velocity (ft/s)	X	22.3	21.7
	Y	31.4	28.1
Ridedown Acceleration (g)	X	4.7	5.0
	Y	13.4	10.3
Max. Angle (degrees)	Roll	49.9	13.9
	Pitch	6.6	9.3
	Yaw	64.6	30.4

3.3.3. 24-inch Gap

With the stable performance of the concrete barrier system with an 18-inch gap width. The impact simulation was performed on the system with a 24-inch gap between the barriers. Figure 3.7 shows the 24-inch gap FE model and vehicle setups showing the impact points and impact angles for Test 3-10 (small car) and Test 3-11 (pickup truck).

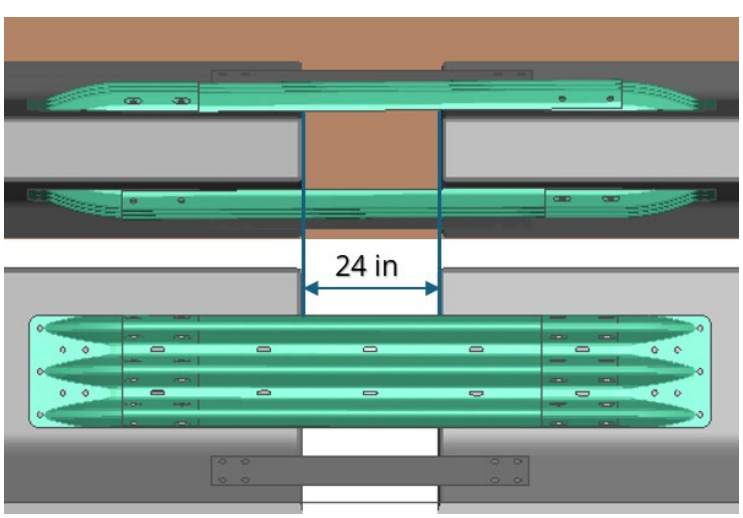

(a) Overview for 24-inch Gap Bridging

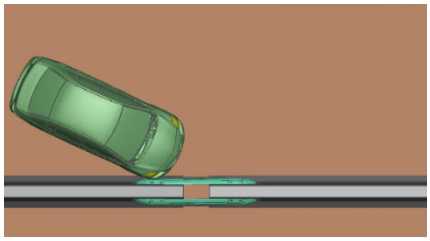

(b) Test 3-10 Simulation Setup

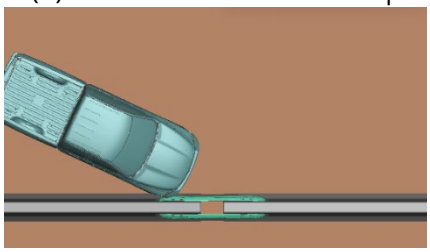

(c) Test 3-11 Simulation Setup

Figure 3.7. Bridging 24-inch Barrier Gap FE Model and Test Simulation Setup

Figure 3.8 and Figure 3.9 show sequential images for the small car and pickup truck, respectively, impacting the 18-inch gap system. Both the small car and pickup truck were effectively contained and redirected by the concrete barriers. Table 3.2 provides the calculated occupant risk factors using TRAP, and results show all occupant risk criteria—impact velocity and ridedown acceleration—were below MASH limits. The 24-inch gap system offered stable vehicle control and maintained strong occupant protection, with only a slight increase in barrier deflection compared to the narrower gap.

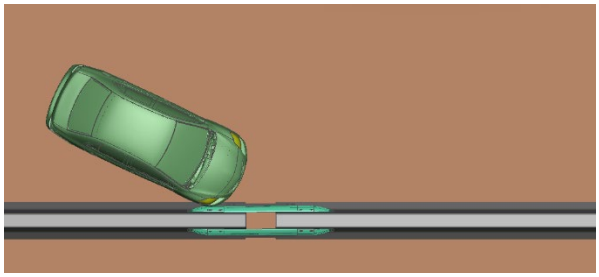

0.00 sec

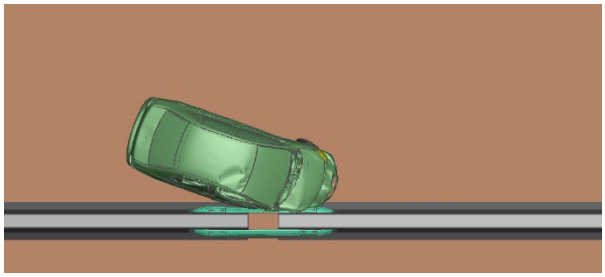

0.07 sec

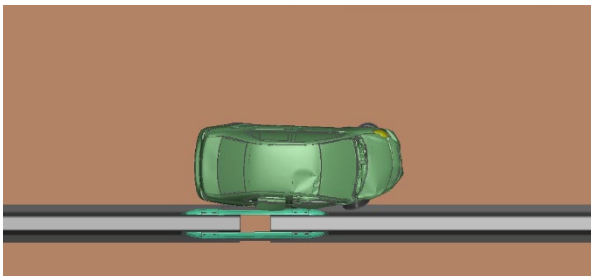

0.14 sec

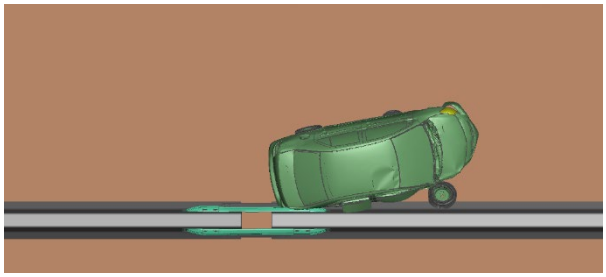

0.21 sec

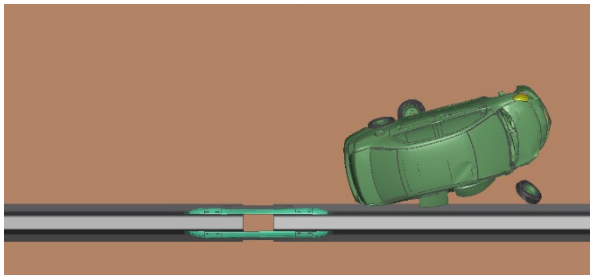

0.28 sec

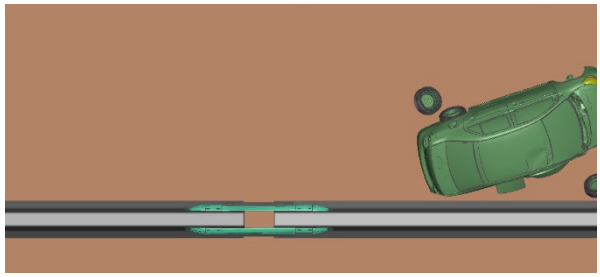

0.35 sec

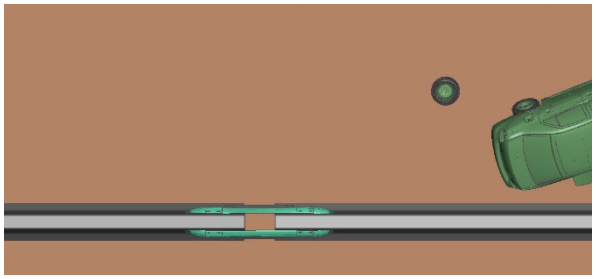

0.42 sec

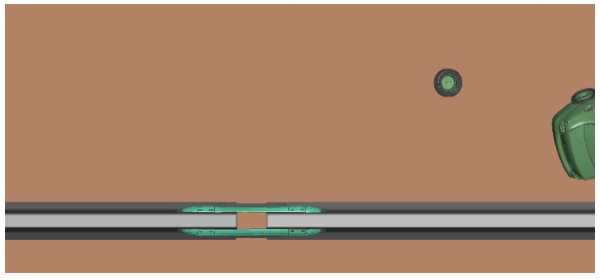

0.49 sec

Figure 3.8. Sequential Images for Test 3-10 Simulation with 24-inch Gap

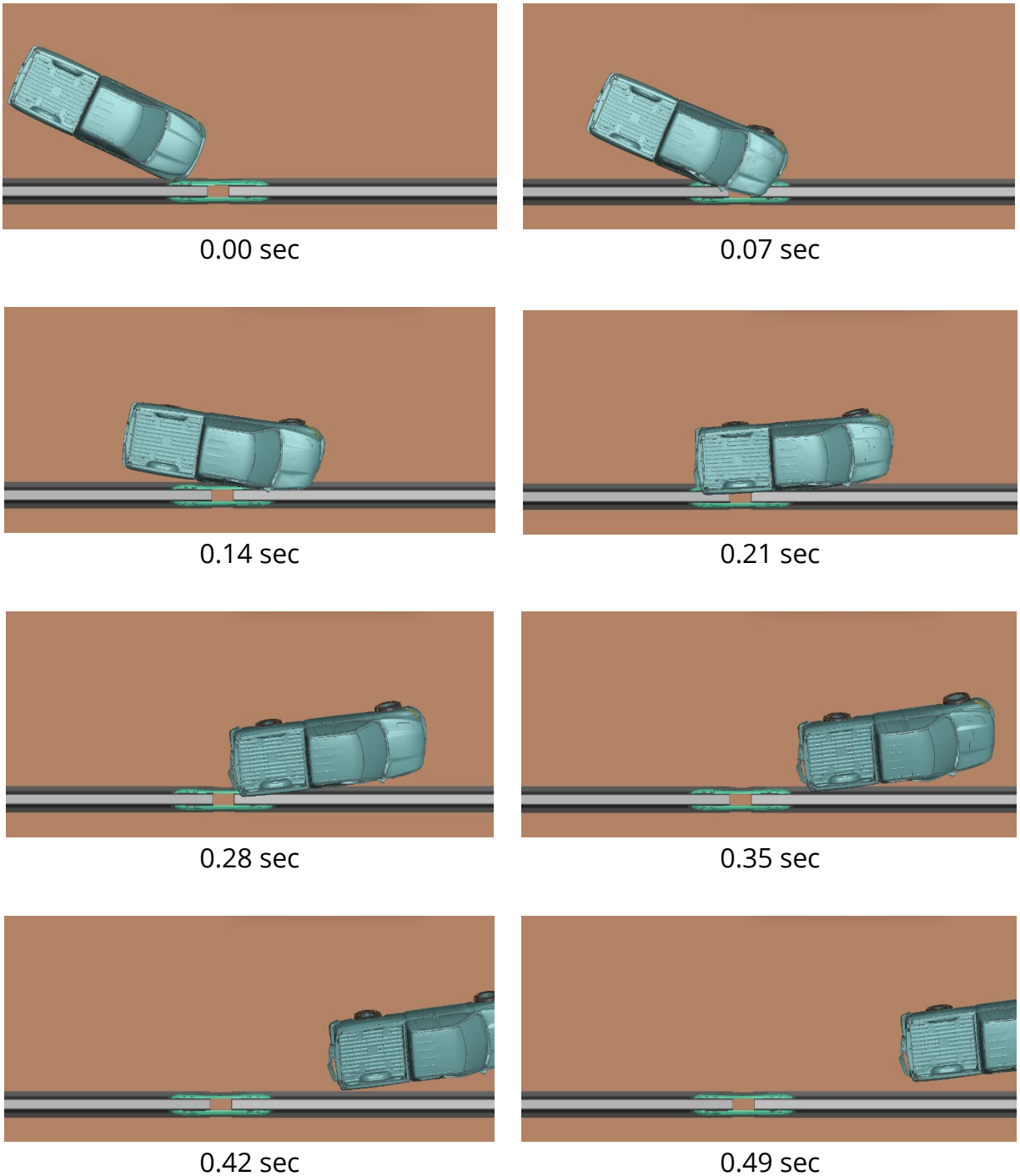

Figure 3.9. Sequential Images for Test 3-11 Simulation with 24-inch Gap

Table 3.2. Occupant Risk Factors for 24-inch Gap Simulation Tests

Occupant Risk Factors		Small car	Pickup Truck
Occupant Impact Velocity (ft/s)	X	20.7	21.7
	Y	31.5	27.9
Ridedown Acceleration (g)	X	4.4	6.6
	Y	12.2	12.6
Max. Angle (degrees)	Roll	19.9	15.8
	Pitch	10.8	7.1
	Yaw	61.9	33.6

3.3.4. 36-inch Gap

Since the stable performance of the 24-inch gap system was observed, the gap was increased by 12 inches (1 ft). The impact simulation was performed on the system with a 36-inch gap. Figure 3.10 shows detailed FE modeling the system with a 36-inch width gap and test simulation setups.

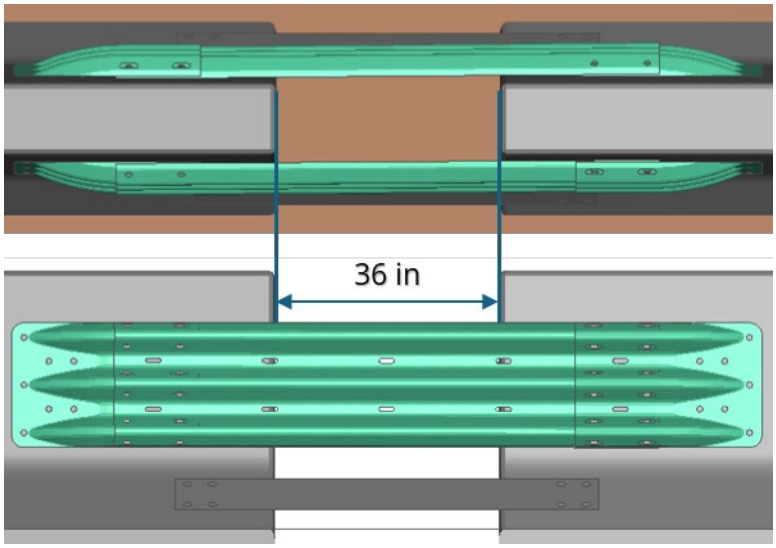

(a) Overview for 36-inch Gap Bridging

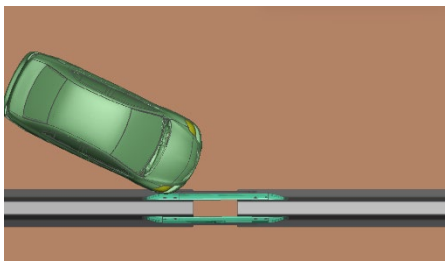

(b) Test 3-10 Simulation Setup

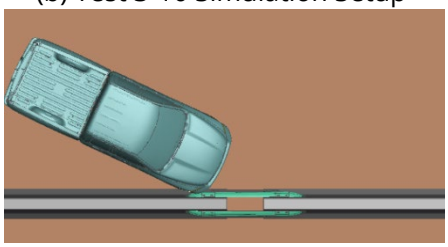

(c) Test 3-11 Simulation Setup

Figure 3.10. Bridging 36-inch Barrier Gap FE Model and Test Simulation Setup

Sequential images are shown in Figure 3.11and Figure 3.12 for the small car and pickup truck test simulations, respectively. Both Test 3-10 (small car) and Test 3-11 (pickup truck) impact simulations resulted in stable containment and redirection of the vehicles. TRAP analysis of the occupant risk factors listed in Table 3.3 indicates all values are within

acceptable MASH criteria. While barrier deflection and vehicle pocketing increased compared to 18- and 24-inch gaps, occupant safety was not compromised at this width.

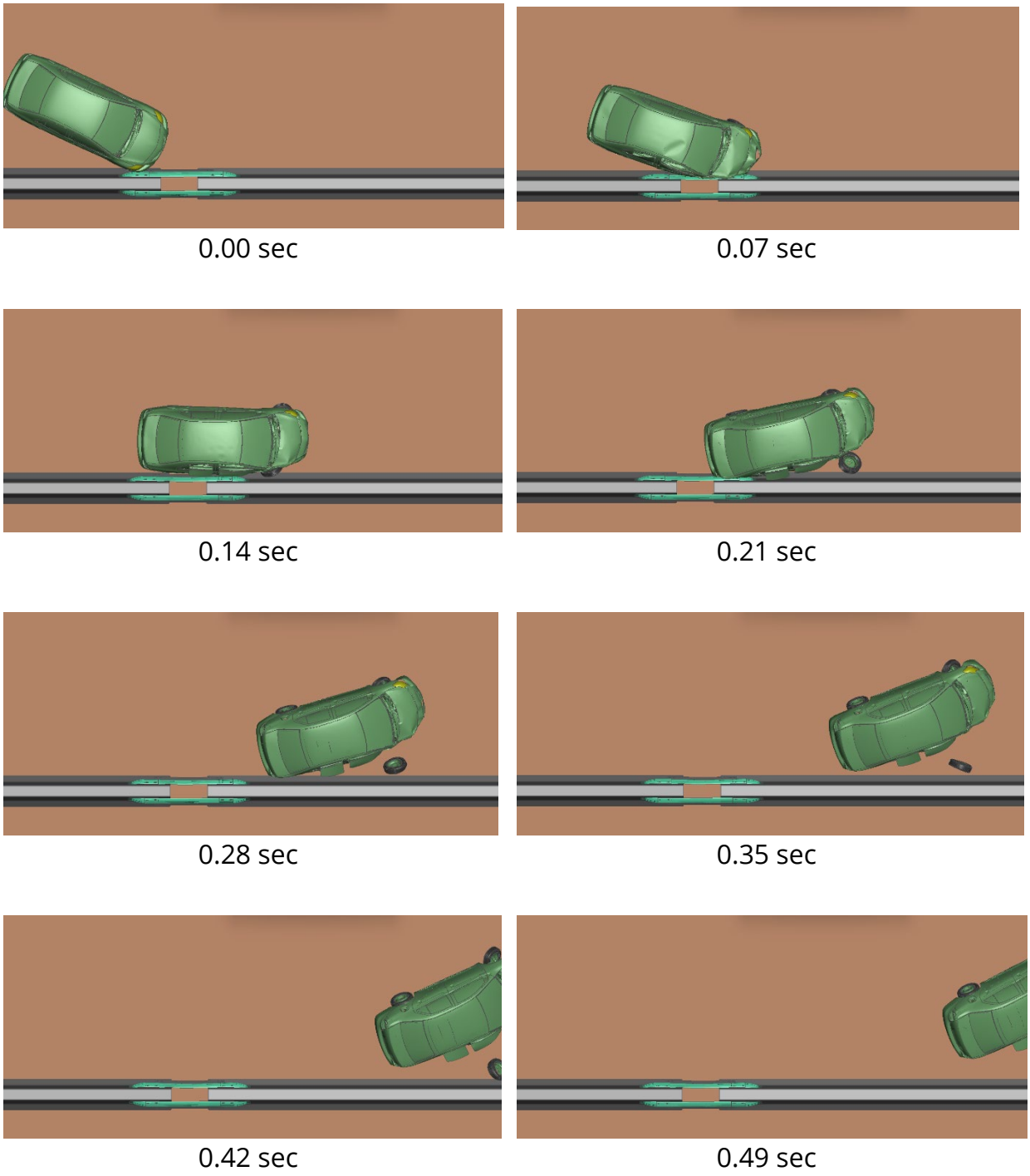

Figure 3.11. Sequential Images for Test 3-10 Simulation with 36-inch Gap

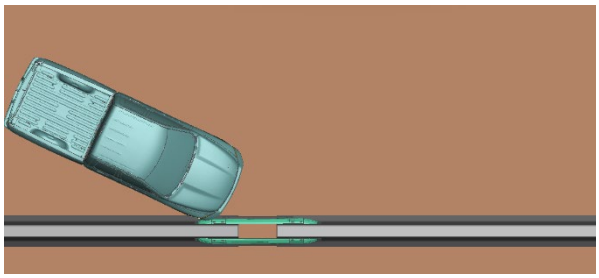

0.00 sec

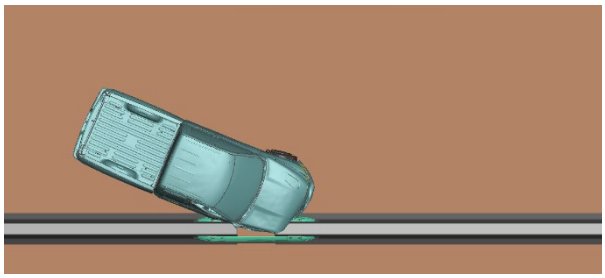

0.07 sec

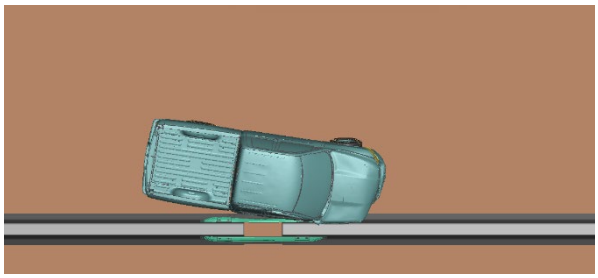

0.14 sec

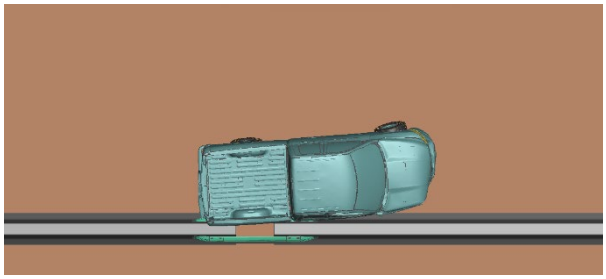

0.21 sec

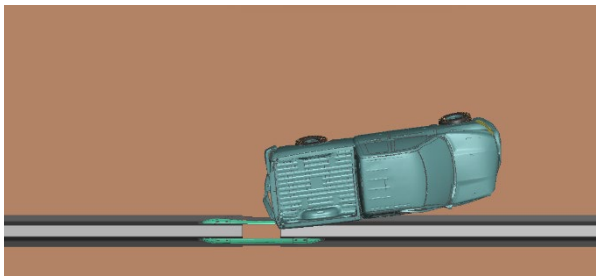

0.28 sec

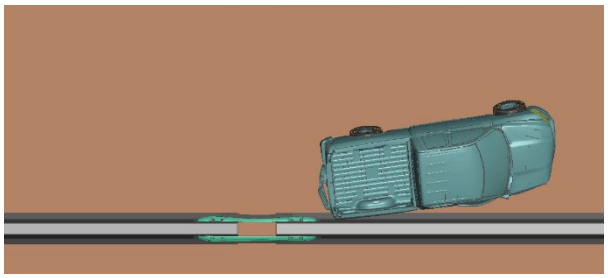

0.35 sec

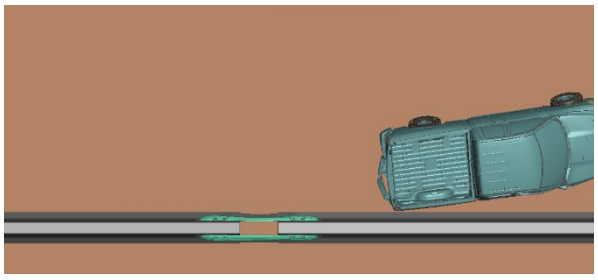

0.42 sec

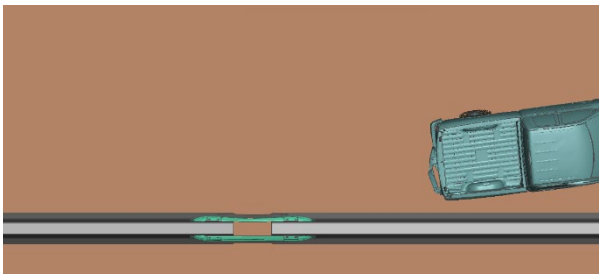

0.49 sec

Figure 3.12. Sequential Images for Test 3-11 Simulation with 36-inch Gap

Table 3.3. Occupant Risk Factors for 36-inch Gap Simulation Tests

Occupant Risk Factors		Small car	Pickup Truck
Occupant Impact Velocity (ft/s)	X	21.9	23.2
	Y	31.7	29.0
Ridedown Acceleration (g)	X	5.3	7.3
	Y	18.9	11.9
Max. Angle (degrees)	Roll	22.7	15.7
	Pitch	10.7	6.8
	Yaw	69.7	34.1

3.3.5. 48-inch Gap

The impact simulation was performed on the system with a 48-inch gap. Figure 3.13 provides the concrete barrier model with a 48-inch gap and test simulation setups.

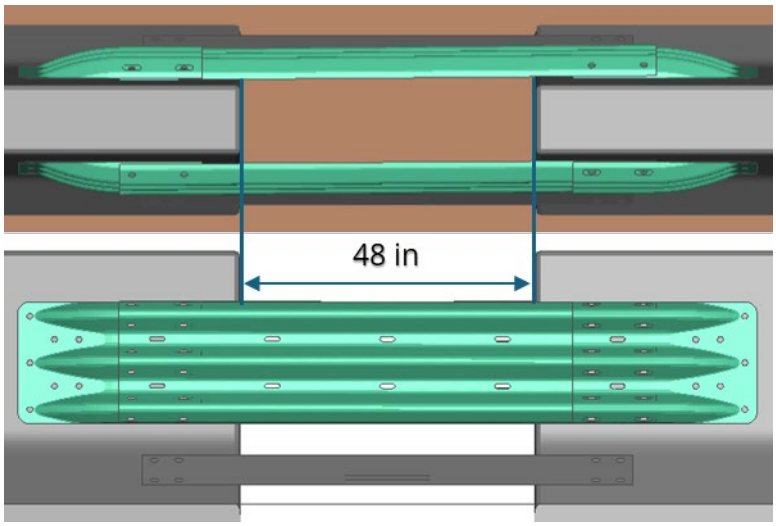

(a) Overview for 48-inch Gap Bridging

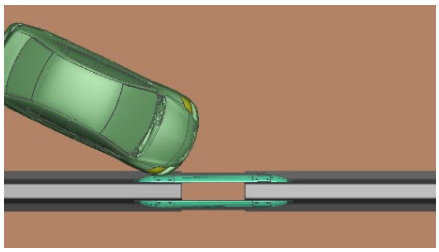

(b) Test 3-10 Simulation Setup

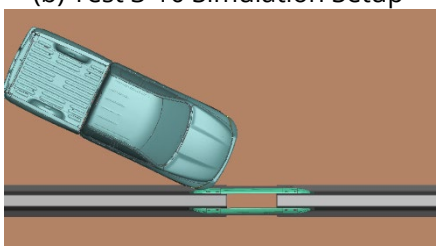

(c) Test 3-11 Simulation Setup

Figure 3.13. Bridging 48-inch Barrier Gap FE Model and Test Simulation Setup

Figure 3.14 and Figure 3.15 illustrate the sequential images for the small car and pickup truck test simulations, respectively. The small car and pickup truck were both stably contained and redirected after collision. Occupant risk factors calculated by TRAP and summarized in Table 3.4 remained below the MASH safety limits. Compared to narrower gaps, barrier deflection and vehicle pocketing became more pronounced, but the system continued to provide acceptable occupant safety and vehicle stability during impacts.

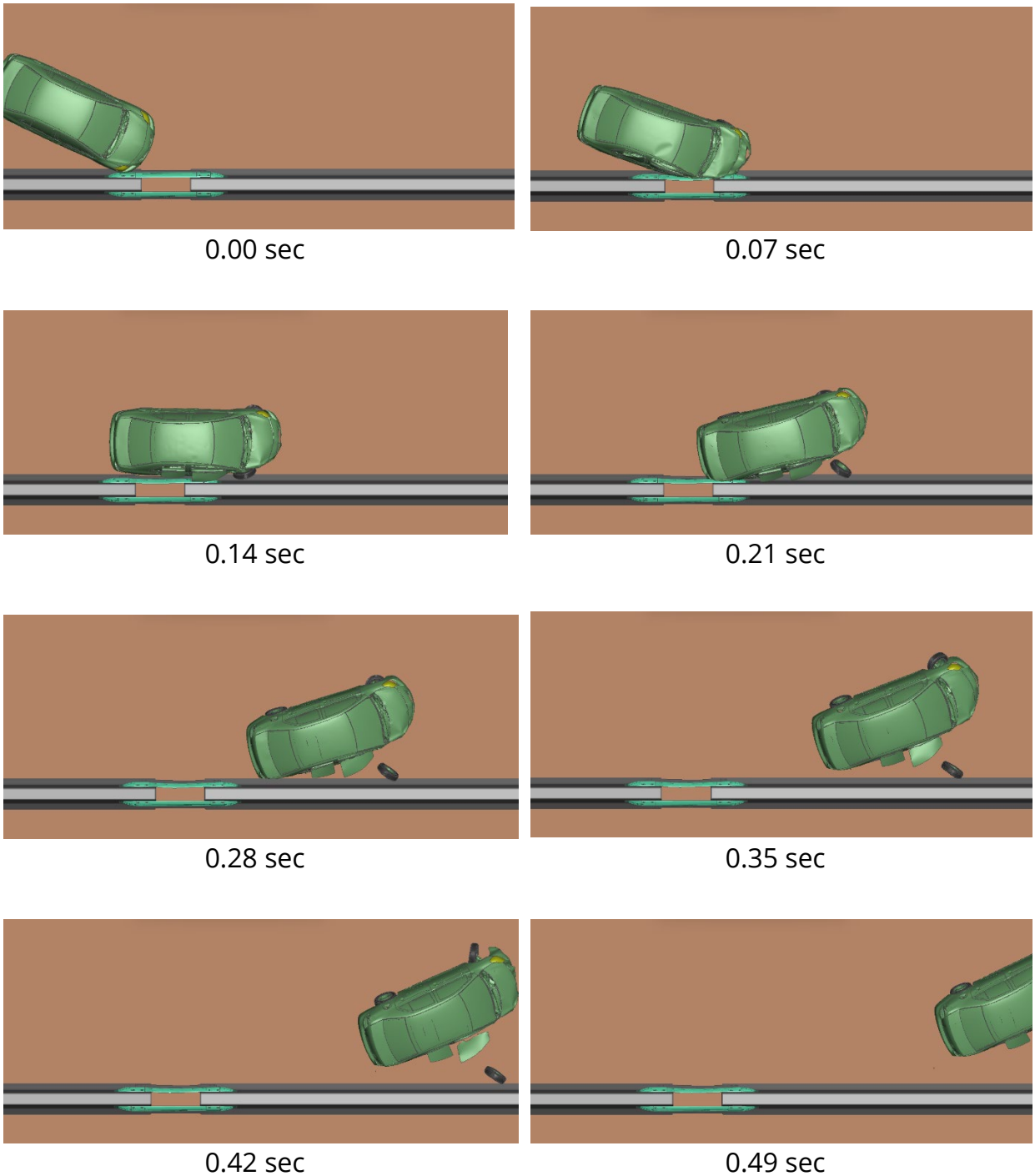

Figure 3.14. Sequential Images for Test 3-10 Simulation with 48-inch Gap

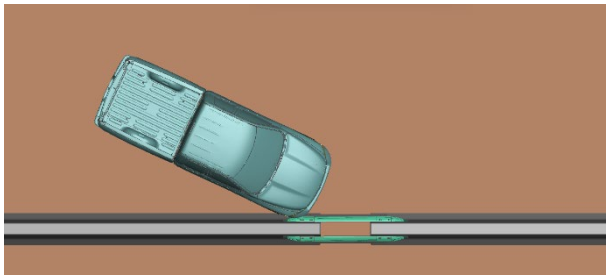

0.00 sec

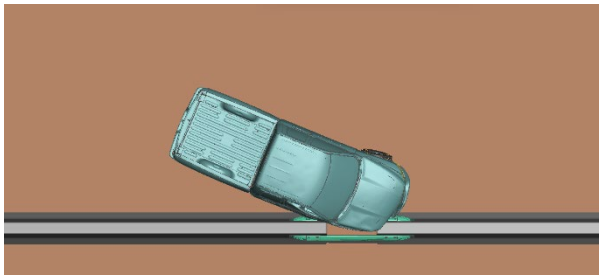

0.07 sec

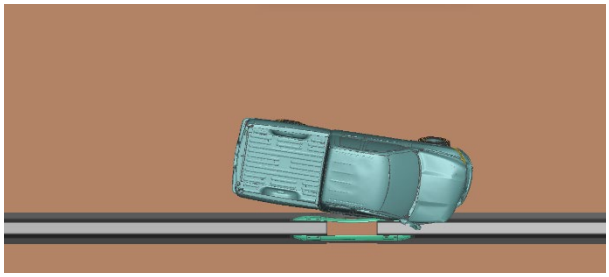

0.14 sec

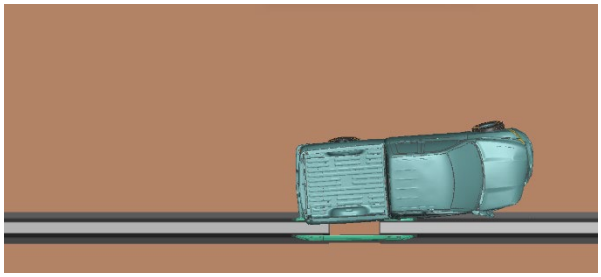

0.21 sec

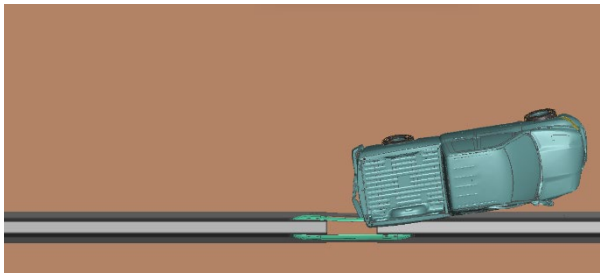

0.28 sec

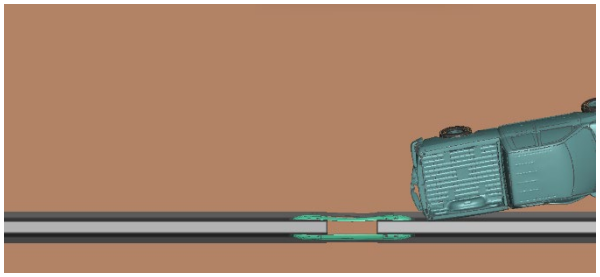

0.35 sec

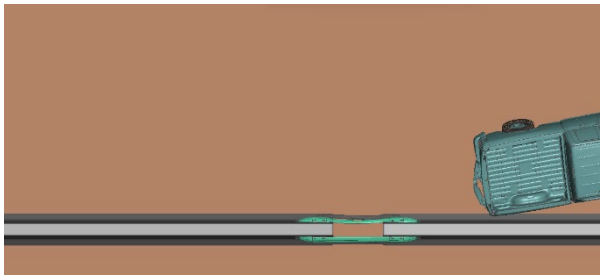

0.42 sec

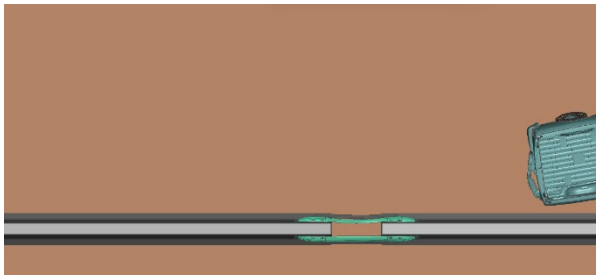

0.49 sec

Figure 3.15. Sequential Images for Test 3-11 Simulation with 48-inch Gap

Table 3.4. Occupant Risk Factors for 48-inch Gap Simulation Tests

Occupant Risk Factors		Small car	Pickup Truck
Occupant Impact Velocity (ft/s)	X	22.2	23.5
	Y	31.6	29.2
Ridedown Acceleration (g)	X	7.4	8.2
	Y	16.0	11.9
Max. Angle (degrees)	Roll	19.5	18.0
	Pitch	10.0	6.7
	Yaw	59.2	35.7

3.3.6. 60-inch Gap

The impact simulation was performed on the system with a 60-inch gap. Figure 3.16 provides the concrete barrier model with a 60-inch gap and test simulation setups.

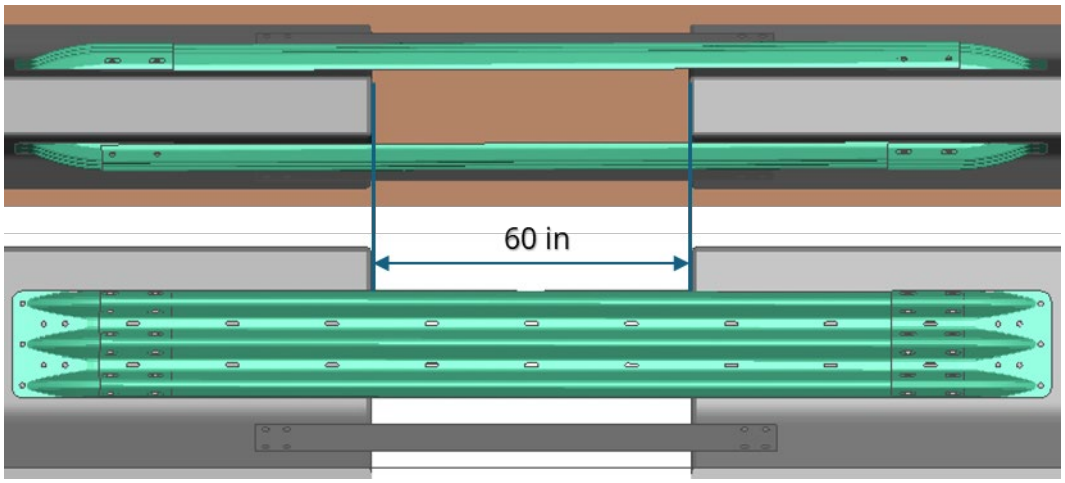

(a) Overview for 60-inch Gap Bridging

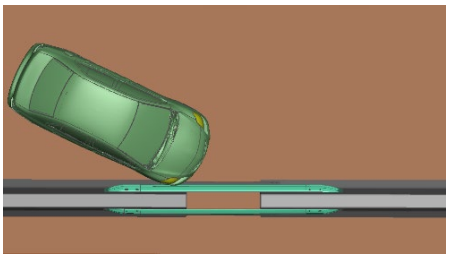

(b) Test 3-10 Simulation Setup

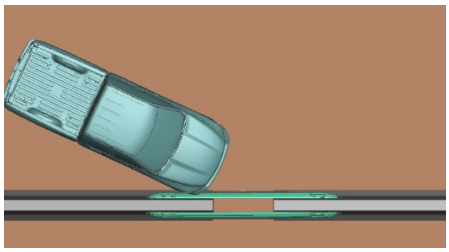

(c) Test 3-11 Simulation Setup

Figure 3.16. Bridging 60-inch Barrier Gap FE Model and Test Simulation Setup

As shown in sequential images in Figure 3.17 and Figure 3.18, both vehicles were successfully contained and redirected by the concrete barrier system. TRAP-calculated

occupant risk values (Table 3.5) for both the small car and pickup truck were below the MASH limits. Although barrier deflection and pocketing were higher and the likelihood of snagging increased when comparing to the system with a 48-inch gap, all occupant risk factors met MASH safety criteria at this gap.

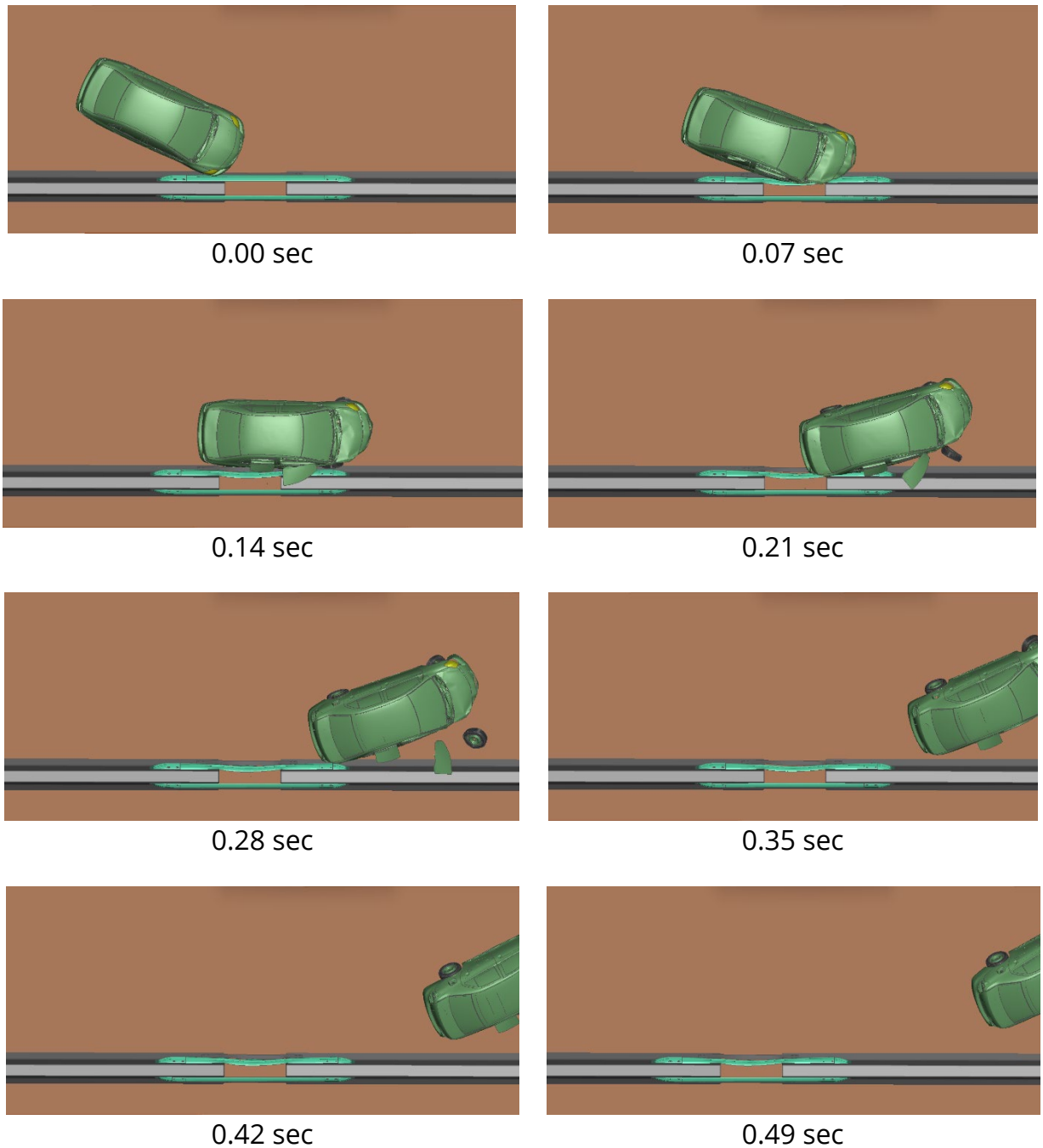

Figure 3.17. Sequential Images for Test 3-10 Simulation with 60-inch Gap

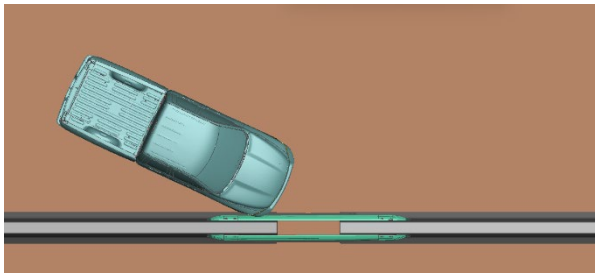

0.00 sec

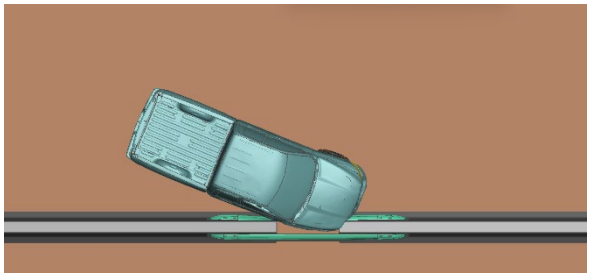

0.07 sec

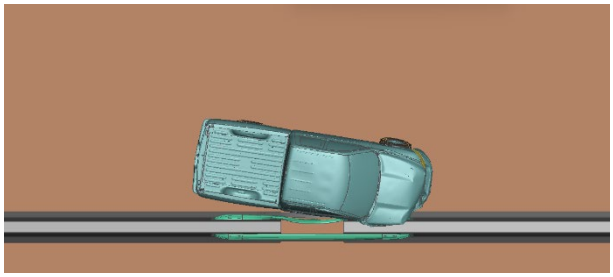

0.14 sec

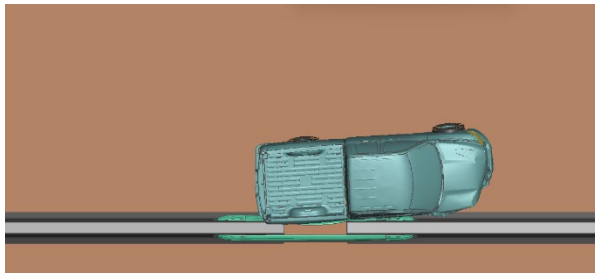

0.21 sec

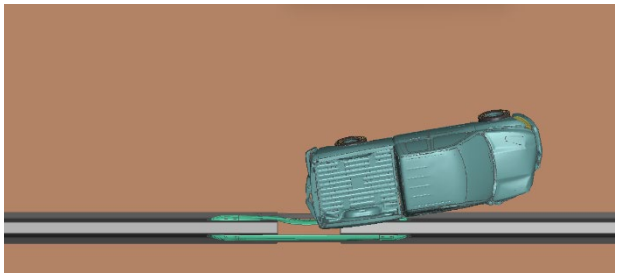

0.28 sec

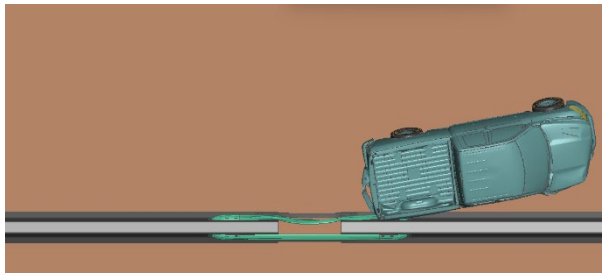

0.35 sec

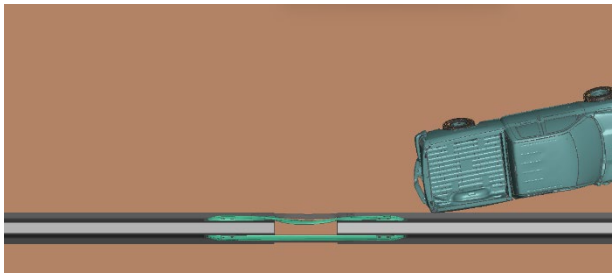

0.42 sec

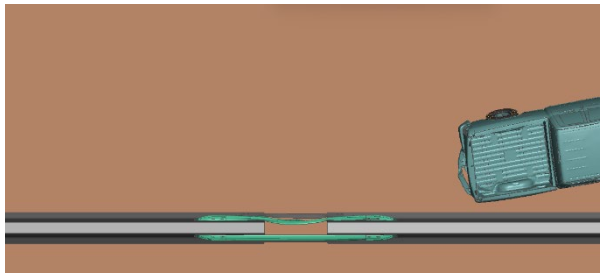

0.49 sec

Figure 3.18. Sequential Images for Test 3-11 Simulation with 60-inch Gap

Table 3.5. Occupant Risk Factors for 60-inch Gap Simulation Tests

Occupant Risk Factors		Small car	Pickup Truck
Occupant Impact Velocity (ft/s)	X	22.2	22.4
	Y	32.1	27.9
Ridedown Acceleration (g)	X	16.2	13.5
	Y	15.1	9.5
Max. Angle (degrees)	Roll	28.1	18.2
	Pitch	13.7	10.1
	Yaw	57.3	36.3

3.3.7. 72-inch Gap

The impact simulation was performed on the system with a 72-inch gap. Figure 3.19 provides the concrete barrier model with a 72-inch gap and test simulation setups.

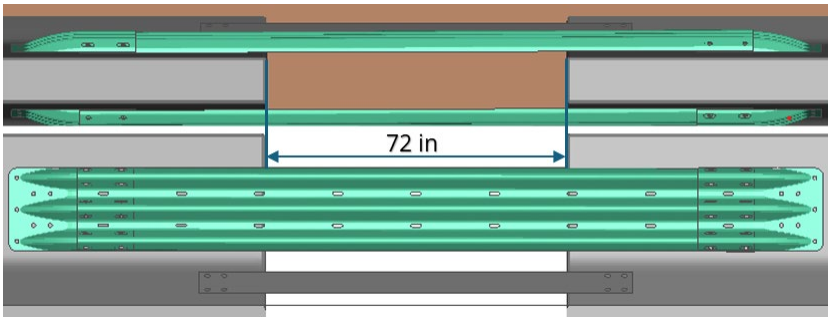

(a) Overview for 72-inch Gap Bridging

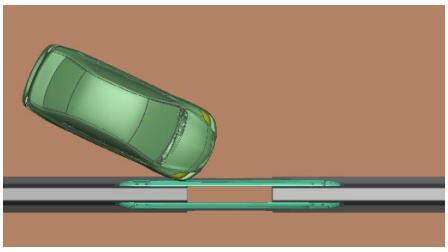

(b) Test 3-10 Simulation Setup

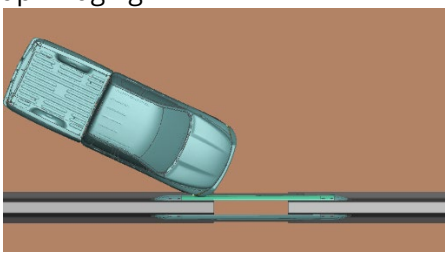

(c) Test 3-11 Simulation Setup

Figure 3.19. Bridging 72-inch Barrier Gap FE Model and Test Simulation Setup

As shown in Figure 3.20 and Figure 3.21, both the small car and pickup truck were technically contained and redirected by the barrier system. While occupant risk values for the pickup truck stayed within MASH limit of 20.49 g, TRAP results for the small car indicated a ridedown acceleration of 25.9g, which exceeds the MASH safety limit and poses significant occupant risk. Barrier deflection and pocketing were at their most severe, and snagging was prominent, emphasizing that the 72-inch gap width may not be suitable for optimal safety, particularly for small vehicles.

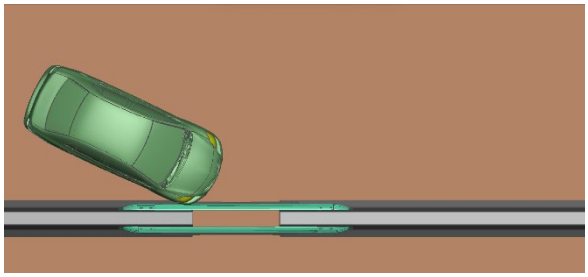

0.00 sec

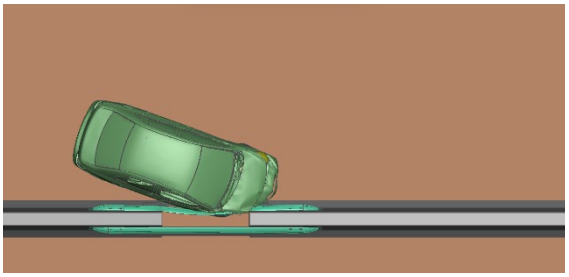

0.07 sec

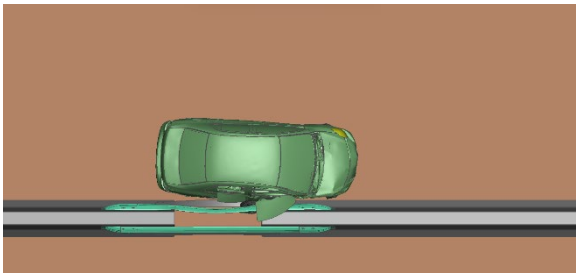

0.14 sec

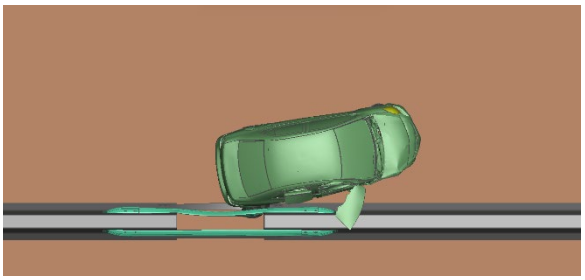

0.21 sec

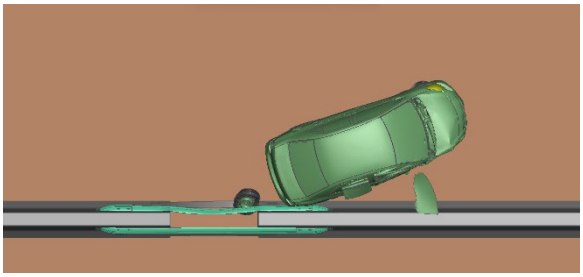

0.28 sec

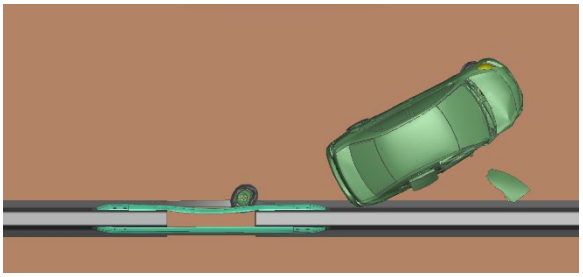

0.35 sec

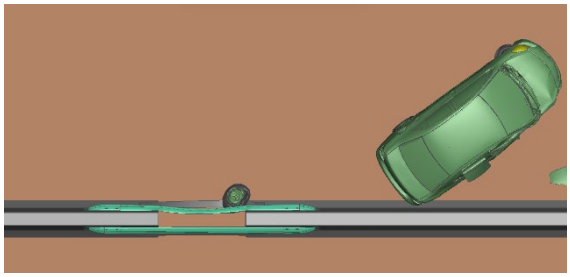

0.42 sec

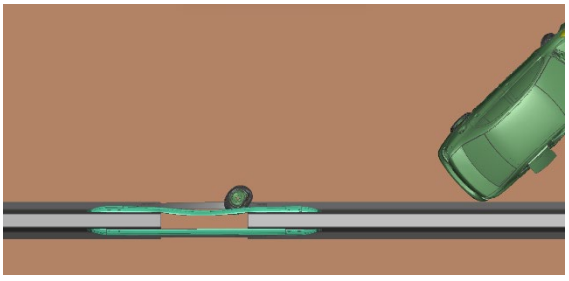

0.49 sec

Figure 3.20. Sequential Images for Test 3-10 Simulation with 72-inch Gap

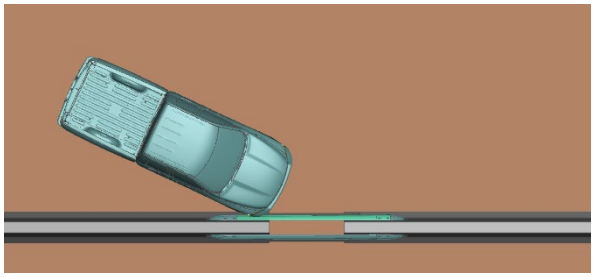

0.00 sec

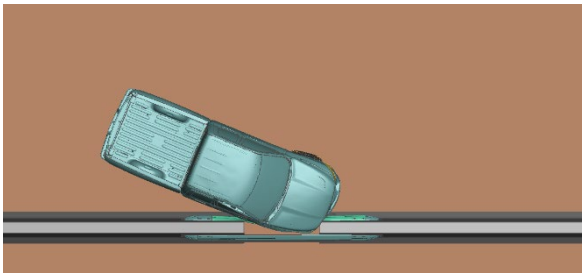

0.07 sec sec

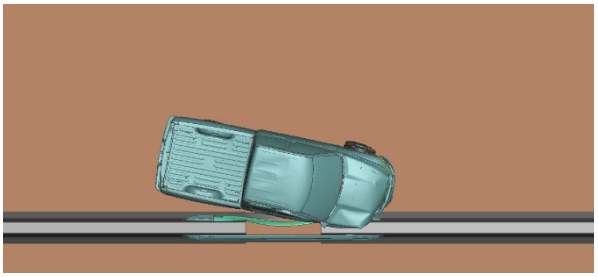

0.14 sec

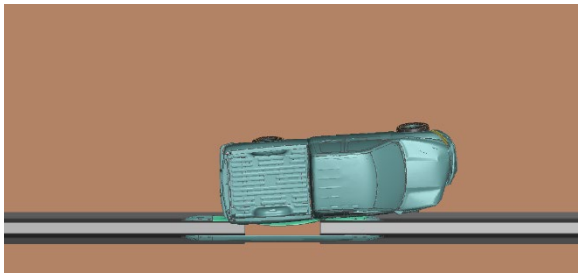

0.21 sec

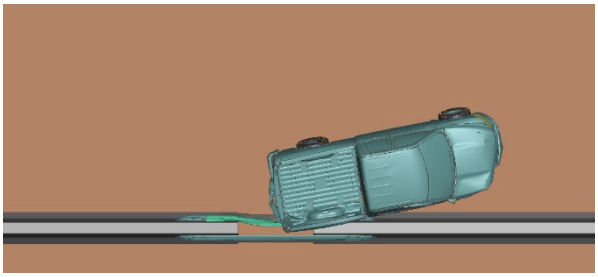

0.28 sec

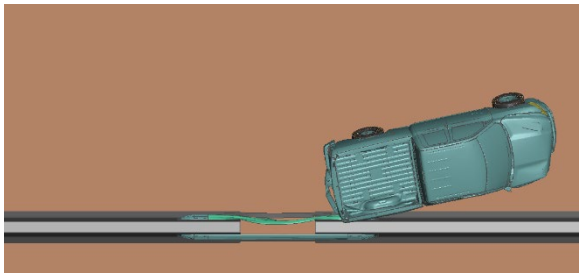

0.35 sec

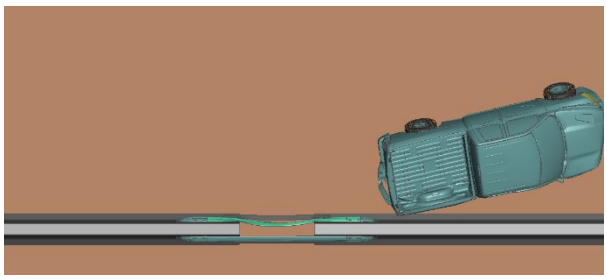

0.42 sec

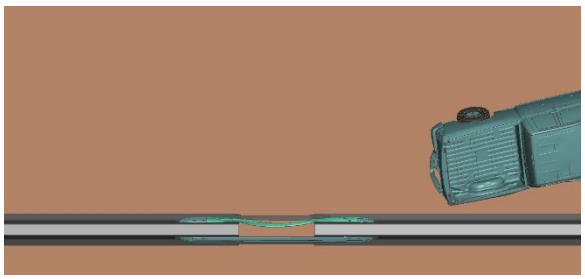

0.49 sec

Figure 3.21. Sequential Images for Test 3-11 Simulation with 72-inch Gap

Table 3.6. Occupant Risk Factors for 72-inch Gap Simulation Tests

Occupant Risk Factors		Small car	Pickup Truck
Occupant Impact Velocity (ft/s)	X	22.1	21.7
	Y	31.5	27.7
Ridedown Acceleration (g)	X	25.9	17.9
	Y	9.6	10.6
Max. Angle (degrees)	Roll	37.6	23.2
	Pitch	9.7	14.6
	Yaw	79.6	38.6

Since the system with 72-inch gap could not meet MASH requirements, no further evaluation with wider gap width would not be performed.

CHAPTER 4.

SUMMARY AND DISCUSSION

Concrete barriers are susceptible to damage, resulting in openings that must be promptly repaired, typically using readily available materials such as W-beam guardrails, thrie beam guardrails, and steel plates. These interim solutions are widely adopted by maintenance teams to restore the effectiveness of the barriers and are preferred for their cost-efficiency and ease of installation in the field.

This project was focused on developing a MASH TL-3 compliant design to bridge a gap between concrete barriers and determining the maximum gap width in a concrete barrier that can be safely spanned. The bridging gap design concepts were developed based on the Ontario Tall Wall Median Barrier. The proposed design utilizes a single 12-gauge thrie beam guardrail across the gap in the F-shape concrete barrier, supplemented by a 6-inch steel rub rail plate at the base for enhanced support.

A finite element (FE) model was developed to represent the bridging gap design, configured with a pre-designed gap between barrier segments. Impact simulations were conducted by using LS-DYNA and performed across a series of gap widths (18 inches, 24 inches, 36 inches, 48 inches, 60 inches, 72 inches, etc.) to identify the critical or maximum span that meets MASH evaluation criteria.

Based on simulation results, the proposed system design with various barrier gaps ranging from 18-inch to 72-inch was able to contain and redirect both small car and pickup truck. With the impact simulation data, occupant risk factors were also evaluated for both vehicle types. Table 4.1 provides occupant risk factors for small cars and pickup trucks across varying barrier widths from 18 inches to 72 inches.

Table 4.1. Summary of Occupant Risk Factors

Occupant Risk Factors		18in		24 in		36in		48 in.		60 in		72 in	
		Small car	Pickup Truck	Small car	Pickup Truck	Small car	Pickup Truck	Small car	Pickup Truck	Small car	Pickup Truck	Small car	Pickup Truck
OIV (ft/s)	X	22.3	21.7	20.7	21.7	21.9	23.2	22.2	23.5	22.2	22.4	22.1	21.7
	Y	31.4	28.1	31.5	27.9	31.7	29	31.6	29.2	32.1	27.9	31.5	27.7
ORA (g)	X	4.7	5	4.4	6.6	5.3	7.3	7.4	8.2	16.2	13.5	25.9	17.9
	Y	13.4	10.3	12.2	12.6	18.9	11.9	16	11.9	15.1	9.5	9.6	10.6
Max. Angle (deg.)	Roll	49.9	13.9	19.9	15.8	22.7	15.7	19.5	18	28.1	18.2	37.6	23.2
	Pitch	6.6	9.3	10.8	7.1	10.7	6.8	10	6.7	13.7	10.1	9.7	14.6
	Yaw	64.6	30.4	61.9	33.6	69.7	34.1	59.2	35.7	57.3	36.3	79.6	38.6

For both small car and pickup truck test simulations, occupant impact velocities in both the longitudinal (X) and lateral (Y) directions remain relatively consistent, with pickup

trucks generally experiencing slightly lower velocities compared to small cars. Ridedown acceleration, which reflects the forces experienced by occupants during crash deceleration, shows a tendency to increase with larger barrier widths—especially for small cars in the longitudinal direction—indicating more severe forces at greater offsets. Looking at maximum roll angles, small cars exhibit significantly higher roll values, particularly at wider barriers, suggesting a greater likelihood of vehicle instability or rotation during impact.

With the overall result, it was determined that the maximum gap width that the bridging barrier gap system safely performed under MASH TL-3 conditions was **60 inches. The occupant ride acceleration of 25.9 g's for the MASH 3-10 small car exceeded the MASH Limits for the 72-inch gap width.** Figure 4.1 provides the maximum deflection profiles and the pocketing for small car simulations with 60-inch gap and 72-inch gap systems to show the differences.

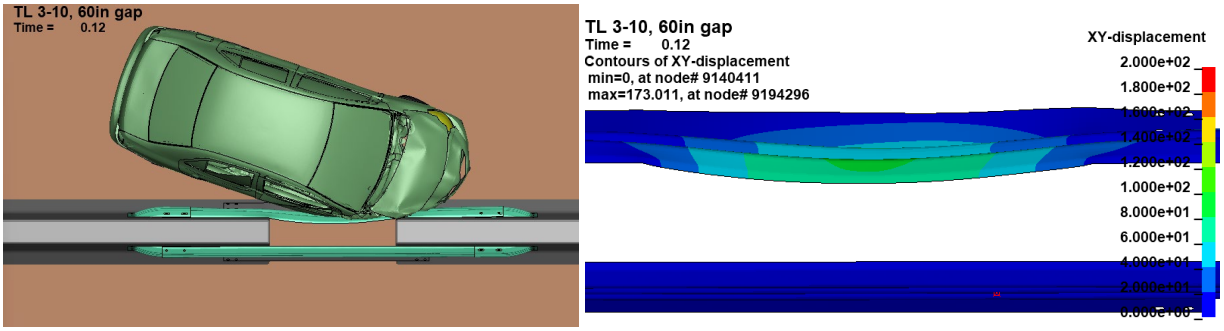

(a) For 60-inch Gap

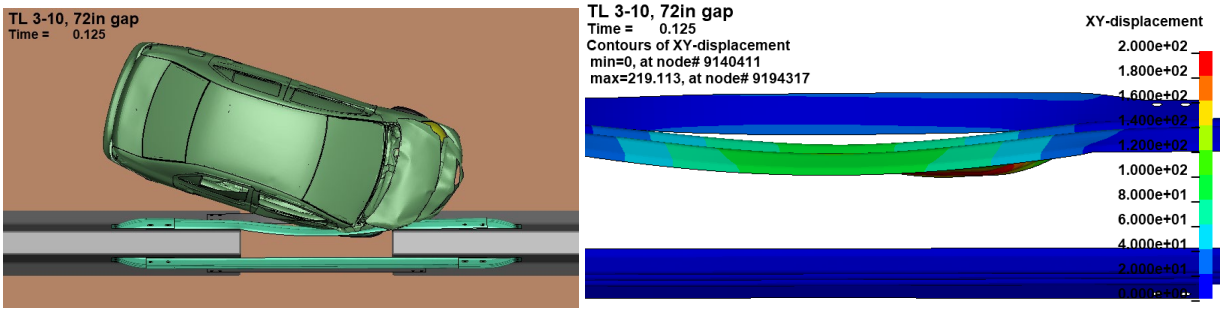

(b) For 72-inch Gap

Figure 4.1. Maximum Deflection and Pocketing for Test 3-10 Simulations

For pickup truck test simulations, although occupant risk factors were under MASH limits, more beam deflections and pocketing behaviors were observed than those for small car test simulations. Therefore, with deflection and pocketing behavior, the potential tear on the beam was also investigated for the pickup truck simulation. Since the FE model was developed without thrie-beam rail failure, potential rail rupture was investigated based on the rail strain. Figure 4.2 shows the rail strain after the impact simulation with 60-inch gap and 72-inch gap systems. Elements with a strain larger than 20 percent are shown in red, so the red regions indicate potential rupture locations. Although the potential rail rupture

in a thrie-beam is lower than that in a W-beam, there is still a chance of rail rupture in the thrie-beam for a 72-inch gap system when it was impacted by a pickup truck.

For the pickup truck test simulations, occupant risk factors remained within MASH limits; however, greater beam deflections and pocketing behavior were observed compared to the small car test simulations. Consequently, the assessment of potential beam tearing was incorporated into the pickup truck simulation. As the FE model was developed without allowing for thrie-beam rail failure, potential rail rupture was evaluated based on the rail strain results. Figure 4.2 presents the rail strain distributions following impact simulations for both 60-inch and 72-inch gap systems. Elements exhibiting strain values exceeding 20 percent are highlighted in red, indicating possible localized tear locations. While the likelihood of rail rupture for thrie-beam systems is generally lower than that for W-beam systems, the results indicate that rail rupture initiated by localized tear in the thrie-beam remains possible for the 72-inch gap configuration subjected to pickup truck impact.

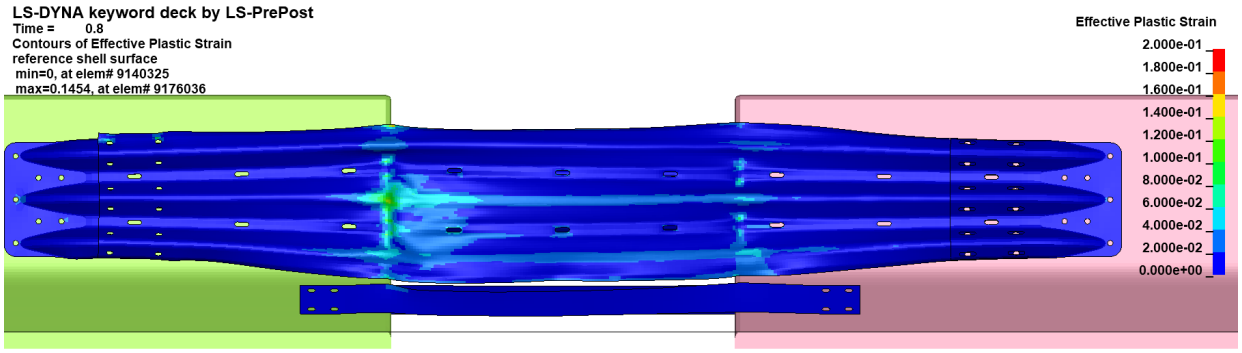

(a) For 60-inch Gap

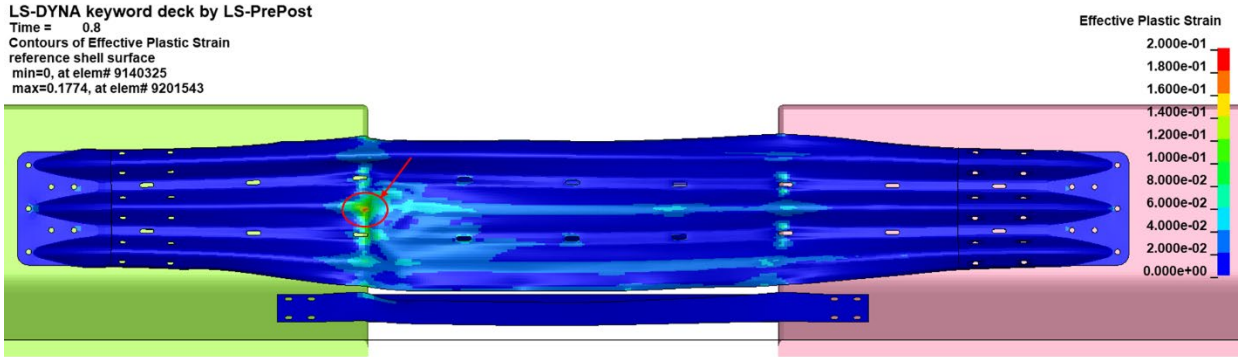

(b) For 72-inch Gap

Figure 4.2. Plastic Strain Predicting Potential Tear in Steel Parts

Based on the simulation results and in accordance with MASH evaluation criteria, the 60-inch barrier gap is recommended as the critical case for the full-scale test. While the 72-inch gap reveals worst-case scenario data, the excessive ridedown

acceleration for the small car makes it unsuitable for regulatory full-scale crash testing under MASH guidelines. The 60-inch gap was acceptable for the occupant risk factors for MASH TL-3 and were within accepted limits for both vehicle types. For this reason, the 60-inch gap design presented herein is recommended for the full-scale test as the most critical and valid case for both MASH 3-10 (small car) and MASH 3-11 (pickup truck).

REFERENCES

1. AASHTO. *Manual for Assessing Safety Hardware*, Second Edition. American Association of State Highway and Transportation Officials, Washington, DC, 2016.
2. Livermore Software Technology Corporation*. LS-DYNA 9 [Version 14.1.0]*. Retrieved from http://www.lstc.com. 2024.
3. Wiebelhaus, M.J., Terpsma, R.J., Lechtenberg, K.A., Faller, R.K., Sicking, D.L., Bielenberg, R.W., Reid, J.D., and Rohde, J.R. *Development of a Temporary Concrete Barrier to Permanent Concrete Median Barrier Approach Transition*. MwRSF Research Report No. TRP-03-208-10. Midwest Roadside Safety Facility (MwRSF), University of Nebraska-Lincoln. 2010.
4. Rosenbaugh, S.K., Schmidt, J.D., Regier, E.M., and Faller, R.K. *Development of the Manitoba Constrained-Width, Tall Wall Barrier.* MwRSF Research Report No. TRP-03-356-16. Midwest Roadside Safety Facility (MwRSF), University of Nebraska-Lincoln. 2016.
5. Ranjha, S.A., Asadollahi Pajouh, M., Bielenberg, R.W., Rosenbaugh, S., and Faller, R.K. *Development of a PCB Steel Cover Plate for Large Open Joints – Phase I*. MwRSF Research Report No. TRP-03-387a-21. Midwest Roadside Safety Facility (MwRSF), University of Nebraska-Lincoln. 2021.
6. Bickhaus, R.F., Bielenberg, R.W., Rosenbaugh, S.K., Faller, R.K., and Ranjha, S.A. . *Development of a PCB Steel Cover Plate for Large Open Joints – Phase II*. MwRSF Research Report No. TRP-03-387b-20. Midwest Roadside Safety Facility (MwRSF), University of Nebraska-Lincoln. 2020.
7. Perry, B.J., Wilson, T.T., Bielenberg, R.W., and Faller, R.K. *Modification and Evaluation of the Asphalt Pin Tie-Down for F-Shape PCB: Test No. WITD-4.* MwRSF Research Report No. TRP-03-488-24. Midwest Roadside Safety Facility (MwRSF), University of Nebraska-Lincoln. 2024.
8. Center for Collision Safety & Analysis. 2018 Dodge Ram 1500 FE Coarse Mesh Model v3 – Validation, Presentation. http://doi.org/10.13021/4p7w-a040. 2022
9. Center for Collision Safety & Analysis. 2010 Toyota Yaris Finite Element Model Validation Coarse Mesh. http://doi.org/10.13021/G8JS5D. 2016.
10. Texas A&M Transportation Institute. *Test Risk Assessment Program (TRAP) [Version 2.5.2].* Retrieved from https://github.com/ttitamu/TRAP. 2024.

APPENDIX A.

DETAILED DRAWINGS

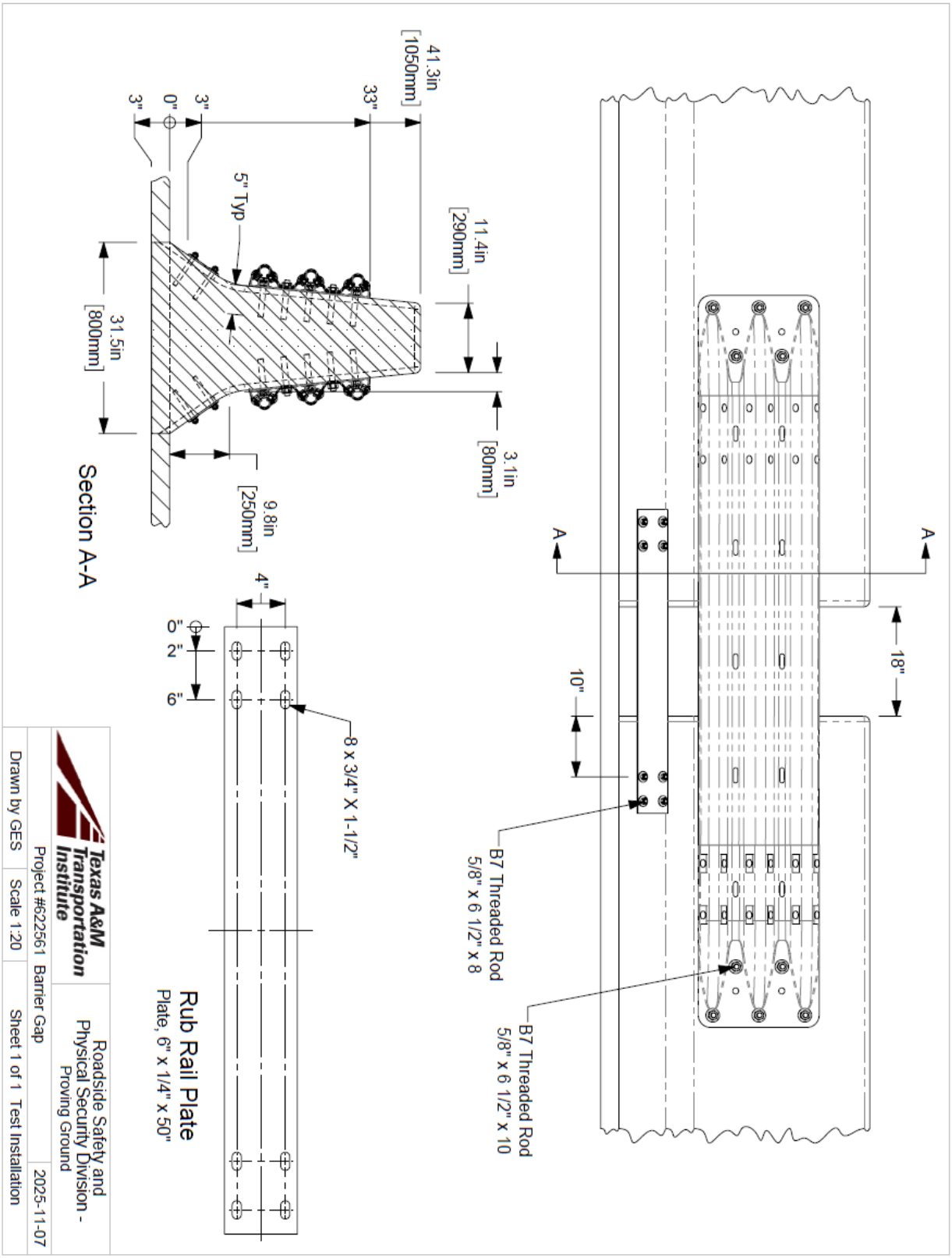

Figure 4.3. Bridging 18-inch Gap Concrete Barriers